BACHELOR'S THESIS

DESIGN OF POLYMERIC HYDRATE INHIBITORS AND KHI PERFORMANCE TESTING

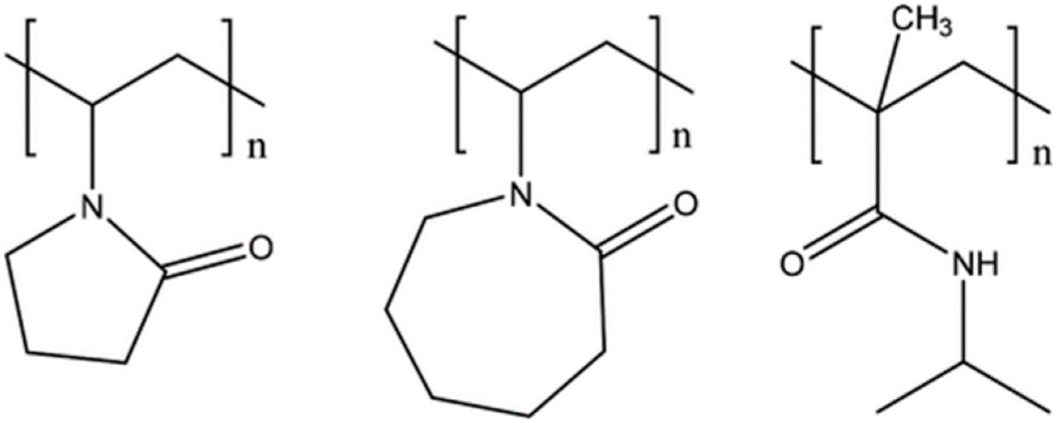

By Ajla Salihovic
Spring 2024

ACKNOWLEDGEMENTS

I would like to thank my supervisor Malcolm Andrew Kelland, for giving me the opportunity to work with him on this thesis and for his guidance, teaching, and professional support during this semester.

I would also like to thank Janronel Calog Pomicpic for helping in the laboratory and introducing the procedures to the different machines used.

I would like to thank my lab partner Julie Kiær for cooperation on the projects, teaching, and a new friendship.

Lastly, I want to thank my family and friends for their patience and support.

SUMMARY

Low dosage hydrate inhibitors are an economical alternative to thermodynamic inhibitors, like ethanol and glycols, to prevent the occurrence of gas hydrates in gas and oilfields. A class of low dosage inhibitors, kinetic hydrate inhibitors, have been commercially used in the field for over 15 years. The developments and search for new and better kinetic hydrate inhibitors is still an ongoing process.

This thesis describes how a high pressure rocking cell, RC5, can be used to test the KHI performances and rank them based on effectiveness and efficiency.

The first part of this thesis is the Poly (2-dialkylamine-2-oxazoline) polymers, a new subclass of amphiphilic polymers. These polymers were made by Richard Hoogenboom and his research team in Belgium, hence why it`s called the “Hoogenboom” project. They were delivered to us for testing their KHI performances.

The second part of this thesis is the PVAmOx-syntheses. These products were made from scratch using different molecular weighted Lupamines as the base. The KHI performance was tested after the syntheses was made. Several polyamine oxides have been investigated as KHIs, and several of them we made showed good KHI performance.

Both the Poly (2-dialkylamine-2-oxazoline) and PVAmOx-reactions were tested with different volumes, concentration, synergists were used, and different gases.

TABLE OF CONTEST

.....1
ACKNOWLEDGEMENTS 2
SUMMARY 3
1 INTRODUCTION 6
2 THEORETICAL BACKGROUND 8
2.1 Gas Hydrates and Structures 8
2.1.1 Structure I 9
2.1.2 Structure II 9
2.1.3 Structure H 10
2.2 Gas Hydrate Formation 10
2.2.1 Hydrate nucleation 10
2.2.2 Hydrate crystal growth 11
2.3 Gas Hydrate Control and Dissociation 12
2.4 Gas Hydrate Inhibitors 13
2.4.1 Thermodynamic Hydrate Inhibitors 13
2.4.2 Anti-Agglomerants 15
2.4.2.1 Pipeline AAs 15
2.4.2.2 Gas-well AAs 15
2.4.3 Kinetic Hydrate Inhibitors 16
2.4.3.1 Factors affecting KHI performance 18
2.4.3.2 Performance testing of KHIs 20
3 MATERIALS AND METHODS 21
3.1 Solutions and Chemicals 21
3.2 Rocking Cell RC5 22
3.2.1 Test procedure 25
3.3 Cooling Method 27
3.3.1 Constant cooling method 27
3.3.2 Isothermal method 28
3.3.3 The ramping method 28
3.4 Gas Hydrate Onset Temperature 28
3.5 Rapid Gas Hydrate Formation Temperature 29
4 EXPERIMENTAL WORK 30
4.1 The “Hoogenboom” Project 30
4.2 Polyvinyl Amine Oxides syntheses 31

4.2.1 Original synthesis of Polyvinyl(R) Amine Oxide 32
4.2.1.1 Separation of Two Layers 32
4.2.1.2 Rotavap and Second Stage 33
4.2.1.3 Testing 34
4.2.2 Polyvinyl(Dipropyl) Amine Oxide 35
4.2.3 Polyvinyl(Dipentyl) Amine Oxide 35
4.2.4 High Molecular Weight Polyvinyl(Dibutyl) Amine Oxide 36
4.2.5 Big Batch Low Molecular Weight Polyvinyl(Dibutyl) Amine Oxide 36
4.2.6 Middle Molecular Weight Polyviny(Dibutyl) Amine Oxide 37
4.2.7 Polyvinyl(Dibutyl) Amine Oxide with 1.5 mol NaOH and BuBr and Heptane Extract 37
4.2.8 Polyvinyl(Dibutyl) Amine Oxide with $NaHCO_3$ 38
4.2.9 Polyvinyl(Dibutyl) Amine Oxide with Acenonitrile 39
4.2.10 Polyvinyl(Dibutyl) Amine to Polyvinyl(tributyl) Amine 39
4.2.11 Monobutylated Polyvinyl Amine Oxide 40
4.3 Other syntheses 40
4.3.1 Synthesis of N-isopropyl-3-(isopropylamino) Propanamide(SAM3i) 40
4.3.2 Lupamin Vacc Down 41
5 RESULTS 42
5.1 PVAmBu_2O vs. H_2O and PVCap 42
5.2 PVAmBu_2O and different mW Lupamin 42
5.3 Poly (2-dialkylamino-2-oxazoline) vs. H_2O and PVCap 43
5.4 Synergists 43
5.5 Poly (2-dialkylamine-2-oxazoline) in SNG and Methane 44
5.6 PVAmBu_2O in SNG and Methane 44
6 DISCUSSION AND CONLUSION 45
REFRENCES 46

1 INTRODUCTION

Gas hydrates, crystalline compounds composed of water molecules hosting gas molecules in their structure, have garnered significant attention in recent years due to their widespread occurrence and potential implication for various fields, including energy exploration, climate change, and offshore engineering (Carroll 2009). Compared to fluid hydrates with specific gravities of 0.8 or less, the gravity of the hydrate solid is typically 0.9. This higher density leads to a problem of ensuring hydrate safety and preventing loss of property or lives (E. Dendy Sloan 2003).

The stability of gas hydrates is influenced by various factors, including temperature, pressure, gas composition and pore space characteristics of the surrounding sediment. Figure 1.1 shows an example of the temperature and pressure equilibrium curve of gas hydrate formation. On the right-side region of the gas hydrate equilibrium curve, no gas hydrate is present, while the left-side region of the equilibrium curve is where gas hydrates can form. The sub-cooling degree equals to the equilibrium temperature (T_{eq}) minus the operating temperature, at a given pressure. Usually, subcooling indicates how far the operating temperature is into the hydrate stability zone.

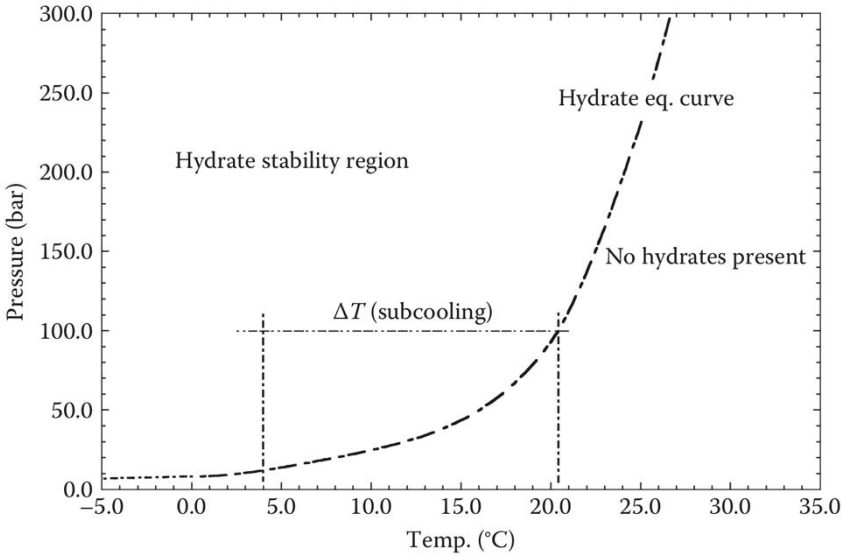

Figure 1.1Pressure-temperature graph for a typical natural gas hydrate.

The prevention of gas hydrates formation is crucial in various industrial applications, particularly in offshore drilling and transportation of natural gas through pipelines. Therefore, many methods to avoid hydrate plug formation have been developed. These include heating, insulation, water removal and the use of chemical inhibitors (Kashchiev and Firoozabadi 2002). Since the early 1990s low dosage hydrate inhibitors (LDHIs) have attracted more and more attention, as the effective dosage of LDHIs required is in much smaller quantities than that of traditional thermodynamic hydrate inhibitors (THI), which is beneficial for capital and operating expenses saving as well as for health and environment protection. Kinetic hydrate

inhibitors (KHI) and anti-agglomerants (AAs) are classified as low dosage hydrate inhibitors. Thermodynamic inhibitors, such as salts and glycols, function by altering the phase behavior of water, lowering the equilibrium temperature and pressure at which gas hydrates form. Kinetic inhibitors impede the nucleation and growth of gas hydrate crystals, thereby preventing their formation. Anti-agglomerants disrupt the agglomeration of gas hydrate crystals, minimizing the formation of hydrate plugs in pipelines.

The new class of hydrate inhibitors can lead to substantial cost saving, not only the reduced cost of the new inhibitor, but also for the size of the injection, pumping and storage facilities (Kelland, Svartås et al. 1995). The promise of LDHIs has been to provide a viable alternative of THIs such as methanol and glycol (Mehta, Hebert et al. 2002). These chemicals have been rapidly adopted in the field and provided a fertile research era for molecular modeling.

While THIs are used in concentrations up to 60wt%, the concentrations of LDHIs are typically 0.1-1.0wt% based on the water phase (Kelland 2006). Methanol (CH_3OH) and monoethylene glycol (MEG, $HOCH_2CH_2OH$) are widely used THIs used to protect against gas hydrate formation in production, workover, process operations and for melting hydrate plugs (Kelland 2009).

KHIs are chemical substances that prevent gas hydrate plugging of oil and gas production flow lines (Kelland, Hoogenboom et al. 2024). The most important, and main, ingredient in KHI formulation is one or more water-soluble amphiphilic polymers. Most of the polymers used as KHIs have multiple amphiphilic groups, where amide, lactam or amine oxide groups usually are the hydrophilic parts of the polymer. KHIs inhibit the hydrate formation process kinetically, either at the nucleation stage or at the crystal growth stage. However, some KHIs have shown to cause complete hydrate dissociation within the gas hydrate-stable pressure-temperature region (Kelland, Hoogenboom et al. 2024).

The focus on this bachelor is to explore the KHI performances of polymers sent from Belgium, as well as making different versions of PVAmine oxides and exploring the KHI performance of these and comparing them to the KHIs we know of today. We had multiple polymers imported from Belgium, by Richard Hoogenboom, whom we tested at different concentrations and volumes, and in both synthetic natural gas (SNG) and in methane. The second project of this thesis was the PVAmine oxide syntheses; here we made different PVAmine oxides with different substances, but PVAmBu_2O was mainly made and tested.

2 THEORETICAL BACKGROUND

2.1 Gas Hydrates and Structures

Gas hydrates are clathrates in which cage-like water molecules form a hydrogen bonded network enclosing roughly spherical cavities that are filled with gas molecules (Figure 2.1). These cages are occupied by small molecules, such as small hydrocarbons, which stabilize the clathrate structure through Van der Waals interactions (Kelland 2009) and capillary forces (Anklam, York et al. 2008). However, gas hydrates are stable as long as 70% of the water cavities are filled with gas molecules, which means some of the water cavities in gas hydrate can be empty.

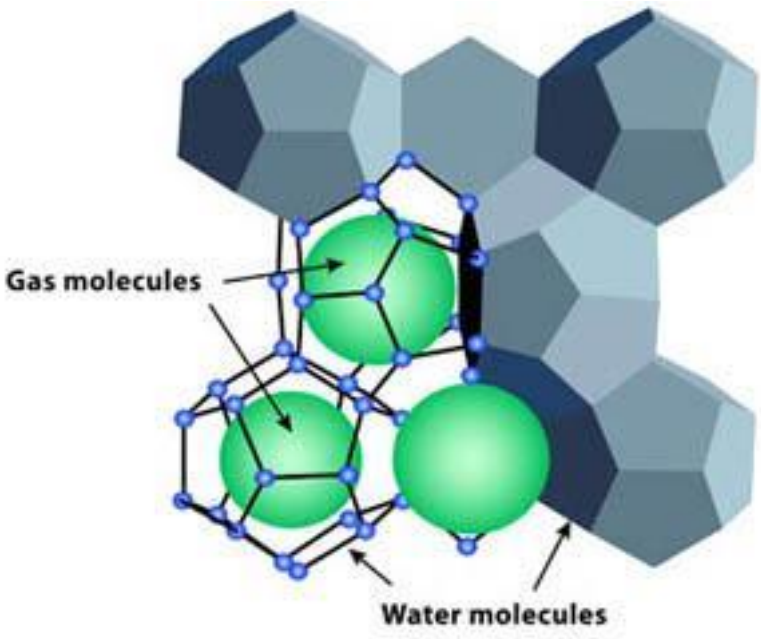

Figure 2.1 Example of cage-like water molecules trapping gas molecules.

The first to report about natural gas hydrates was Sir Humphrey Davy in 1810, while in 1934 it was first documented by Hammerschmidt about gas hydrates being a problem in natural gas pipes (Sloan and Koh 2008). Since then, the gas hydrate formation and dissociation phenomena have been the subject of numerous studies (Makogon 1997).

Hydrates are formed by hydrogen bonds among water molecules, resulting compounds molecule align to stabilize and precipitate into solid mixture (Báez and Clancy 1994). The formation of gas hydrates is caused by contacting of small so-called “guest” molecules, such as methane and carbon dioxide, with host under optimum temperature and pressure (Sloan 2003). The structure of the lattice composed of cavities which clathrate individual gas molecules. The water lattice is determined by the size of the “guest” molecule and the composition of the gas. The structures of gas hydrates are classified according to the different cavity types of their composition, Figure 2.2.

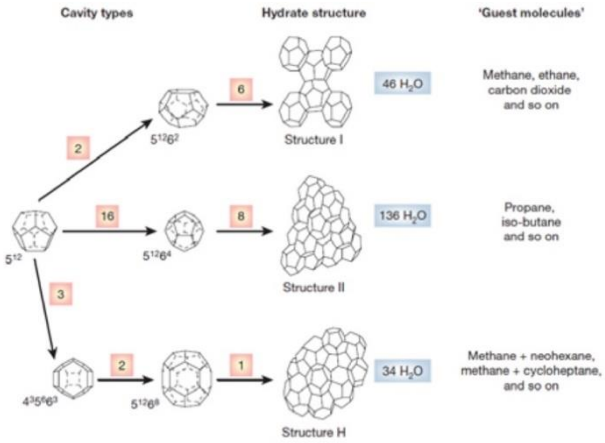

Figure 2.2 Typical structures of gas hydrates.

There are three structures for gas hydrates: the cubic structure I, cubic structure II and the hexagonal structure H, shown in Figure 2.3.

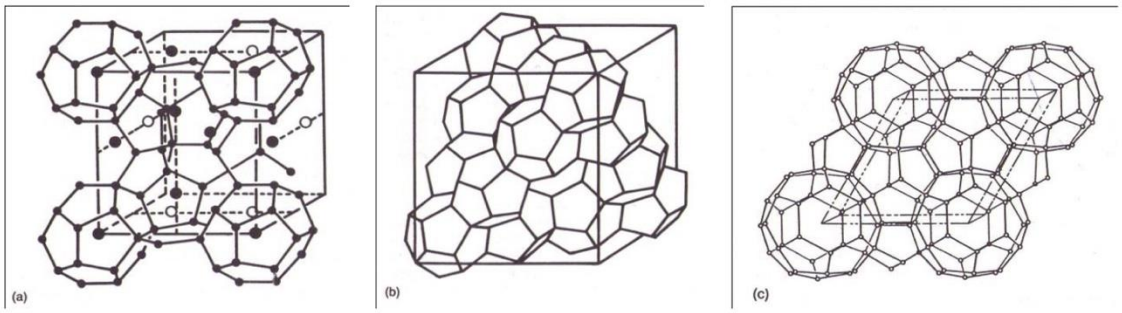

Figure 2.3 The three gas hydrate formations; a) structure I, b) structure II and c) structure H unclose (Sloan and Koh 2008).

2.1.1 Structure I

Structure I (sI) is mostly found in nature because methane is the major component in most of hydrates found outside the pipeline (Sloan 2011). These structures are formed with small molecules (0.4-0.55nm), like with methane, ethane, carbon dioxide and hydrogen sulfide (Sloan and Koh 2008).

2.1.2 Structure II

Structure II (sII) hydrates occurs when somewhat larger molecules are present (0.6-0.7nm), for instance when the natural gas mixture include propane or iso-butane (Sloan and Koh 2008). sII hydrates are mostly found in the gas and oil operating process (Sloan 2011) and is by far the most common hydrate structure found in the field, due to its stability whenever a natural gas mixture contains some propane or butane besides methane (Kelland 2009).

2.1.3 Structure H

Structure H (sH) is more complex than sI and sII. If even larger molecules, (0.8-0.9nm) such as iso-pentane or neohexane, are present in mixture with smaller molecules, like methane, hydrogen sulfide or nitrogen, sH hydrates may form (Sloan and Koh 2008). However, under unusual conditions, such as at very high pressure, they can have multiple cage occupancy with unusually small guest molecules, like hydrogen and noble gasses (Sloan 2003, Mao et. al. 2008).

A^n can be interpreted as, *A* is the face sides number of a cage and *n* is the amount of faces the cage holds.

2.2 Gas Hydrate Formation

Hydrates form at increasing pressure and at lower temperature. It can be seen in Figure 1.1 that the temperature below which hydrates can form increases with increasing pressure (Kelland 2009). Figure 2.4 shows a sketch of areas where hydrate blockages may occur in a simplified offshore deepwater system from the well to the platform export flowline. Hydrate blockages in a subsea flowline system are most likely to be found in areas where the direction of flow changes in the well, pipeline, and riser parts of a system.

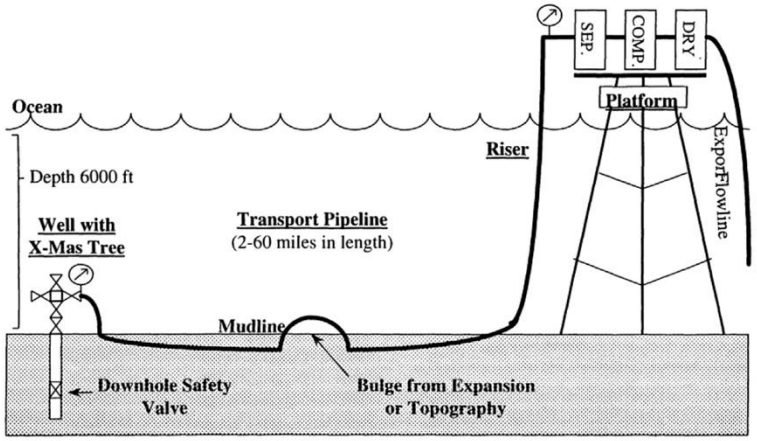

Figure 2.4 Typical offshore well, production pipeline and platform.

2.2.1 Hydrate nucleation

As understood, gas hydrate formation is a time dependent process that can be divided into hydrate nucleation, hydrate growth and dissociation as illustrated in Figure 2.5.

Hydrate nucleation is the process that produces a small labile cluster, called hydrate nuclei. This cluster consists of water and gas molecules. It grows, disperses, and tries to grow further because a labile cluster is unstable and ready for continuous changing (Sloan and Koh 2008). The general formula for hydrate gas formation is expressed by equation below.

$$M\ (g) + nH_2O\ (l) \Leftrightarrow M \times nH_2O\ (s) \quad (1)$$

M is natural gas molecules, *n* is number of water molecules required to form a gas hydrate per one molecule of gas, and $M \times nH_2O$ is gas hydrate (Tang 2010).

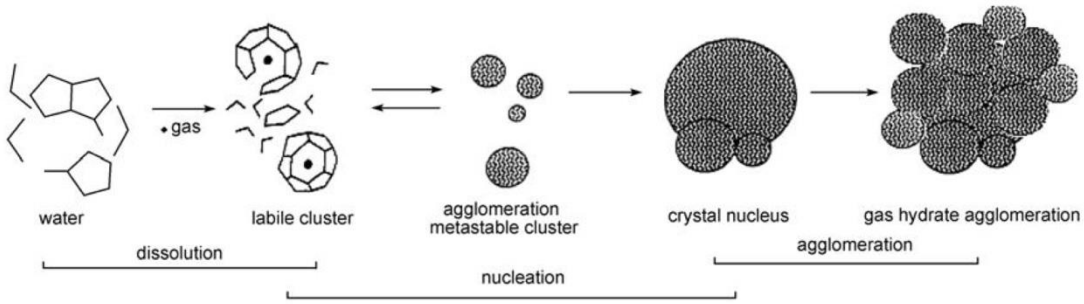

Figure 2.5 Hydrate formation hypothesis

2.2.2 Hydrate crystal growth

The formation of hydrate nucleation is a quite stochastic process, as well as it may happen in nanoseconds with the length scale being nanometers. After hydrate crystal nucleation, the crystal growth process occurs continuity to agglomerate gas hydrate, as seen in Figure 2.5. These are the kinetics of crystal growth at the surface of hydrate, mass transfer components to the growing surface, and heat transfer away from the growing surface. They are also considered major factors of growth process as seen in Figure 2.6, as they carry out constant volume and temperature changes during an experiment. Gas reacts with water in point 1, and after that the pressure reduces linearly with the temperature. There is no hydrate formation during 1st and 2nd period, called induction time, because of metastability (Sloan and Koh 2008). Induction time is defined as the time taken from entering to hydrate forming region and the onset of hydrate formation (Fu, Cenegy and Neff 2001). Hydrate formation begins in point 2. The pressure drops dramatically to point 3, resulting in rapid hydrate growth through the end of growth for hydrate formation. Hydrate dissociation starts, after heat is added to the system, from point 3 to A. This is called the hydrate equilibrium temperature and pressure (Sloan and Koh 2008). As there is limited gas or water components in a reaction vessel, it will eventually reach the solid hydrate stable condition again.

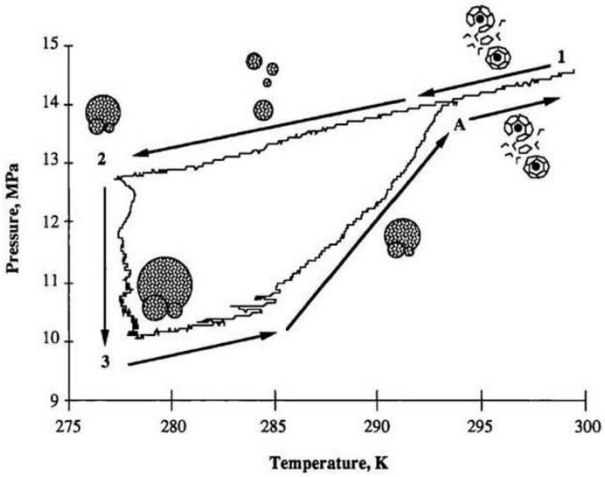

Figure 2.6 Diagram of temperature and pressure trace for methane hydrate formation (Christianses and Sloan 1994).

2.3 Gas Hydrate Control and Dissociation

Gas hydrates are non-flowing crystalline solids, so they are not welcomed during the transportation of gas and oil products. Once a gas hydrate blockage forms, the production stoppage may be required to remove the hydrates, and it costs high capital expense (CAPEX) and operating expense (OPEX). The density of hydrate solids is much larger than that of the fluid hydrocarbon, so the formation of hydrates may damage expensive gas and oil facilities, and it may also cause safety problems. Economic drives for further research on LDHIs as they are a wide range of OPEX savings, possible extended field lifetime and multi-million-dollar CAPEX savings (Kelland 2006). The operation of hydrate blockage removal also comes with the potential of facility damage. Methods for hydrate prevention must be considered, to provide flow assurance, especially for the flow lines in deeper ocean and arctic areas.
Hydrate dissociation is an endothermic and vital process to eliminate hydrate crystal. Thus, decomposition of gas hydrate to water and gas molecules can be successful by supply external heat to destroy hydrogen bond between water molecules and Van der Waals interaction between gas and water molecules (Sloan and Koh 2008). There are different approaches which can be applied to damage limitation a plug of gas hydrate such as:

Water control: removing as much water as possible in the flow lines before the transportation of gas and oil products. This can be by gas dehydration, water separation and water cut reduction (Jr 2003).

Gas management: minimize the gas phase by the application of hydraulic methods, meaning to keep the operational pressure lower than the equilibrium point of gas hydrate formation (Kelland 2006).

Thermal methods: keep the operational temperature high to operate in the no-hydrate region, Figure 1.1 and Figure 2.7. This can be done by direct heating and isolation (Sloan 2005).

Chemical inhibition.

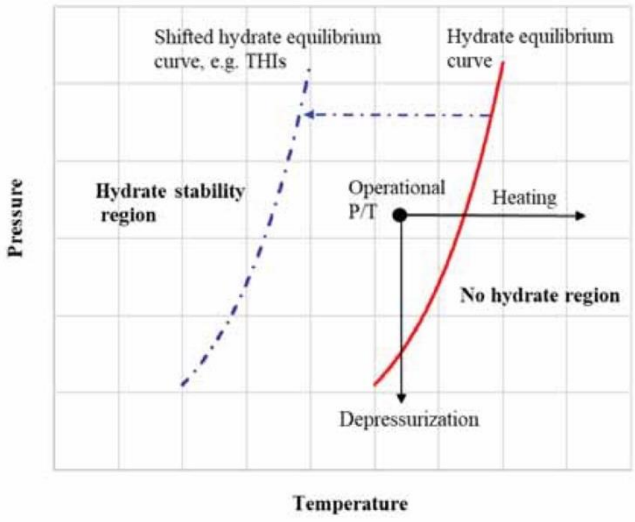

Figure 2.7 Schematic of how THIs, heating and depressurization affect hydrate formation.

All these methods have been used in the oil and gas field, where chemical inhibition is the most common method to prevent and reduce gas hydrate formation. As it is impossible to completely eradicate the water in the production well pipes, the presence of some water is usually inevitable. The methods of heating and insulating flowlines are expensive, especially

for long-distance transportations. A high pressure is usually required to guarantee the production rate.

2.4 Gas Hydrate Inhibitors

Hydrate chemical inhibitors can be divided into two classes: thermodynamic hydrate inhibitors (THI) and low dosage hydrate inhibitors (LDHI) (Sloan 2011). While THI required high concentrations of inhibitors to be successful LDHI operates by using low dosage of inhibitors or agglomerants (Kelland 2009). THIs can shift the equilibrium point of hydrate formation to higher pressure or lower temperature, meaning that THIs can melt the already formed gas hydrates. LDHIs have two branches: kinetic hydrate inhibitors (KHI) and anti-agglomerants (AA). KHIs delay the hydrate formation rate, thus preventing the blockage of hydrates during the gas and oil transportation while AAs enable hydrates to form as small transportable dispersed particles.

The development of LDHIs started in the mid-1900s (Kelland 2006) and have been in commercial use in the upstream oil and gas industry for about 15 years (Kelland 2009). LDHIs are a cost-effective alternative to the traditional THIs (Lovell and Pakulski 2003). Neither KHIs or AAs will change the thermodynamic equilibrium of the hydrates, but rather change the hydrate kinetics and agglomeration, respectively (Kelland 2009). Both branches of LDHIs are successfully used in fields applications (Kelland, Svartås et al. 2008). However, LDHIs are not recoverable, and they are expensive. The difference in hydrate inhibition mechanism between LDHIs and THIs are shown in Figure 2.8 (Bai and Bai 2019).

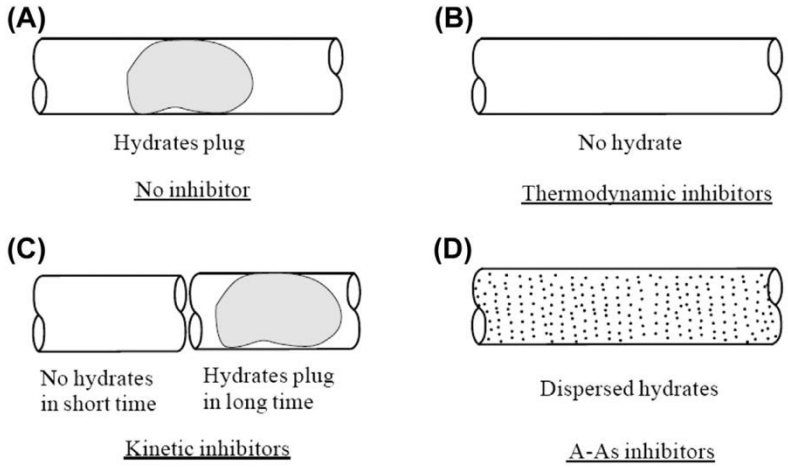

Figure 2.8 Mechanism of hydrate inhibitors.

2.4.1 Thermodynamic Hydrate Inhibitors

Thermodynamic hydrate inhibitors, also known as anti-freeze, are the most common chemical prevention method to use. Typical THIs are alcohols like methanol and ethanol, some inorganic salts, and glycols such as monoethylene glycol (MEG) and diethylene glycol (DEG). They act by modifying the bulk thermodynamic properties of the fluid system. Methanol and MEG are the two most common used THIs. Because of its effectiveness, low cost, and easy availability, methanol is often used to prevent hydrate plugs or to dissociate a hydrate plug that has formed (Giavarini and Hester 2011). Since methanol has a quite low molecular weight, 32 g/mol, some of it vaporizes into the gas phase when used to prevent

gas hydrates from forming in flowlines. Since methanol is highly flammable, toxic, and refinery catalyst-killing, MEG is preferred many places worldwide. Due to its comparatively higher molecular weight, 62 g/mol, it can easy be recovered through the removal of water. However, DEG may be justified as it is easier to recover and better at dehydrating natural gas (Gavarini and Hester 2011).

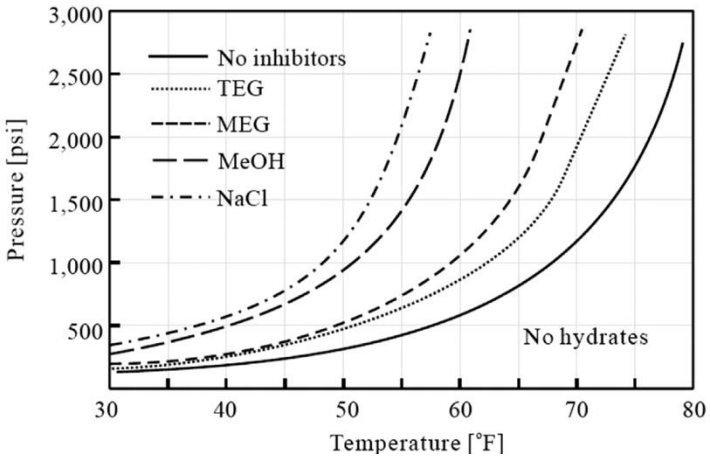

Figure 2.9 Effect of THI on hydrate formation.

Figure 2.9 shows the effect of typical thermodynamic inhibitors on hydrate formation at 20 wt% fraction. Salt, methanol, and glycols act as thermodynamical hydrate inhibitors that shift the hydrate stability curve to the left (Bai and Bai 2019). As seen on the figure salt (NaCl) has the most impact on the hydrate stability temperature. The addition of methanol and MEG acts by preventing the water molecules from participating in the solid hydrate structure but keeps them in the liquid flowable phase. The more inhibitor added to the system, the more water is prevented from participating in the hydrate structure, so higher pressure and lower temperatures are required for gas hydrate formation from the remaining, uninhibited water (Sloan 2011).

By changing the bulk thermodynamic properties of the fluid system, the equilibrium conditions for gas hydrate formation are shifted to lower temperatures or higher pressure (Kelland 2009). However, a high concentration of THIs is required to be effective, ca. 20-80 wt%. The correct dosing of THIs is very important since under-inhibition, at certain dosages, can instead increase the plugging potential (Kelland 2009).

Looking at the overall and longtime expenses for system inhibition are dominated by the regeneration system and makeup costs for inhibitor loss. Even though methanol is cheaper per unit volume, with increasing field life it becomes more expensive due to methanol makeup costs. Because of high volume requirements of THIs, the cost of subsea multiphase transportation over long distance due to storage capacities, injection and regenerations facilities needed are high (Kelland 2009). Thus, the alternative method of utilizing significantly lower concentrations of LDHIs for hydrate preventions becomes attractive (Mehta, Hebert et al. 2002).

2.4.2 Anti-Agglomerants

Anti-agglomerants (AAs) are a type of LDHI. They are surface active chemicals used in pipeline, not in drilling (Sloan and Koh 2008). AAs do not stop hydrates from forming, rather they prevent agglomeration and deposition of hydrate crystals and the consequent formation of plugs, such that a transportable hydrate slurry is formed (Kelland 2006). This action mode makes AAs useful even at higher subcooling conditions in deepwater applications (Kelland 2009).

There are two classes of AAs that are commercially in use: pipeline AAs and gas-well AAs.

2.4.2.1 Pipeline AAs

The application of pipeline AAs requires a liquid hydrocarbon phase to disperse the formed hydrate, and a water cut below 80-90% to ensure that hydrate slurry is not too viscus to transport (Kelland 2006, Webber 2012). There have been proposed two working mechanisms of pipeline AAs: the emulsion mechanism and the “hydrate-philic” mechanism.

The emulsion mechanism, a water-in-oil emulsion can form when injecting a surfactant. Hydrate particles that form within the water droplets of the emulsion cannot easily get agglomerate. In the “hydrate-philic” mechanism, the “hydrate-philic” groups of the amphiphilic surfactants attach to the hydrate surface and disrupt its growth. The hydrocarbon side of the amphiphilic surfactants makes the attached hydrates hydrophobic, even though the small hydrate particles can be easily dispersed in the oil phase (Klomp, Kruka and Reijnhart 1997).

2.4.2.2 Gas-well AAs

Gas-well AAs can disperse hydrate in excess water, and then the small hydrate particles can be transported by the aqueous phase without agglomeration. (Lovell and Pakulski 2002). Thus, the application of gas-well AAs doesn’t require a liquid hydrocarbon phase. Polyetherpolyamines with low molecular, under *500 g/mol*, are excellent gas-well AAs. Figure 2.10 shows an example of Polyetherpolyamines, polyetherdiamine. Polyetheramine gas-well AAs have been used to prevent hydrate blockages in many gas-well applications.

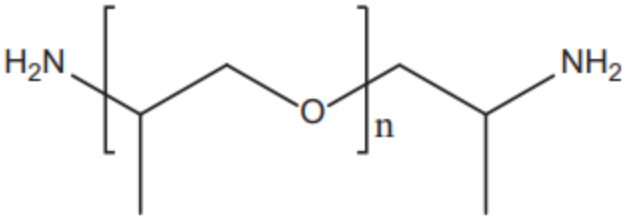

Figure 2.10 Structure of polyetherdiamine gas-well AA

AAs require the presence of liquid hydrocarbon phase to transport the suspension of the converted hydrate crystals, and they cannot be used at high water cuts (Kelland 2009).

2.4.3 Kinetic Hydrate Inhibitors

The high costs of THIs have stimulated the search for KHIs (Lovell and Pakulski 2003).

KHIs are water-soluble polymers. They primarily act as gas hydrate anti-nucleators, although most of KHIs delay the gas hydrate formation for a period depending on the subcooling, and to a less extend the pressure (Kelland 2012). The most common industrial application of KHIs is during upstream oil and gas production in cold flowlines, but they can also be used in drilling and completion fluids, or for subterranean injection of CO_2 to avoid gas hydrate plugging (Sloan and Koh 2008). When evaluating the performance of a KHI the main parameters looked at is the driving force for hydrate formation in a system, and time for hydrate formation. Subcooling (ΔT) is used as an approximate value for the driving force. KHI applications are limited to situations where the subcooling is less than 10-12°C, this is because the delay time above this subcooling becomes too short to safely transport the well fluids for a long pipeline residence time. KHIs allow for transport of hydrate-forming fluids for a certain period before hydrates start to form (Kelland 2006). Since KHIs are a subgroup of LDHIs, a typical dosage is about 1000 – 1500 ppm (0.1 – 0.5 wt%).

KHIs formulation contain one or more water-soluble polymers, which are often synergists to boost the polymer performance. Some of the typical polymers used as KHIs have multiple amphiphilic groups where amide, lactam or amine oxide groups comprise as the hydrophilic part of the polymer. A molecule that is amphiphilic means that it has both hydrophobic and hydrophilic regions. The hydrophobic part is usually a hydrocarbon fragment with 3-6 carbon atoms, which is thought to interact with open cavities on the hydrate particles imitating the alkane gas molecules that would otherwise be trapped in hydrate cages (Kelland, Hoogenboom et al. 2024). The most common and effective KHIs are amide-based polymers, which include:

1. Polymers with amide side groups. Poly (N-vinyl pyrrolidone) (PVP), poly (N-vinyl caprolactam) (PVCap), and poly (N-isopropyl methacrylamide) (PNIPMAM) are some examples.
2. Polymers with amide backbones, such as anti-freeze proteins bespoke polypeptides and pseudo-polypeptides (Reyes, Guo et al. 2014).

PVP was the first KHIs to be discovered in 1991 (Kelland 2006). PVP is a five-ring of the series of polyvinyllactams, and without any synergists it has a subcooling around 3-4°C at 70-90 bar. PVP, PVCap and PNIPMAM have been commercialized in this field, Figure 2.11. PVCap and PVP have been investigated since the early 1990s, and they are still used as standards for evaluating the performances of new KHIs.

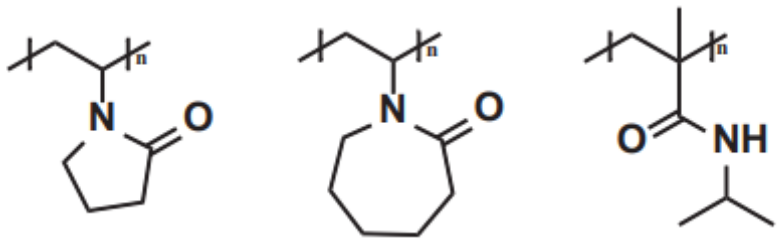

Figure 2.11 Stuctures of PVP, PVCap and PNIPMAM.

The strategy behind the designs of current KHIs originally came from doing research on anti-freeze proteins, Figure 2.12. Anti-freeze proteins are found in some species of fish, insects, plants, and bacteria (Edwards 1993). These types of anti-freeze proteins must not be

confused with antifreezes like glycols, which function different by depressing the freezing point of water. These types of anti-freeze proteins contain polypeptides which bind to small ice crystals to inhibit growth and recrystallization of ice that would otherwise be fatal to species (Kelland 2012). It has been a general assumption that amide groups in anti-freeze proteins bind to the ice crystal surface, limiting and distorting the crystal growth. The requirement is a correct spacing between of the amide groups to align with water molecules on the ice surface. Although some of the amide groups in the anti-freeze proteins can bind via hydrogen bonding to water molecules on the ice crystals, other data suggests that hydrophobic interactions could be the main contribution (Kelland 2012). The development of current KHIs is based on the anti-freeze protein research.

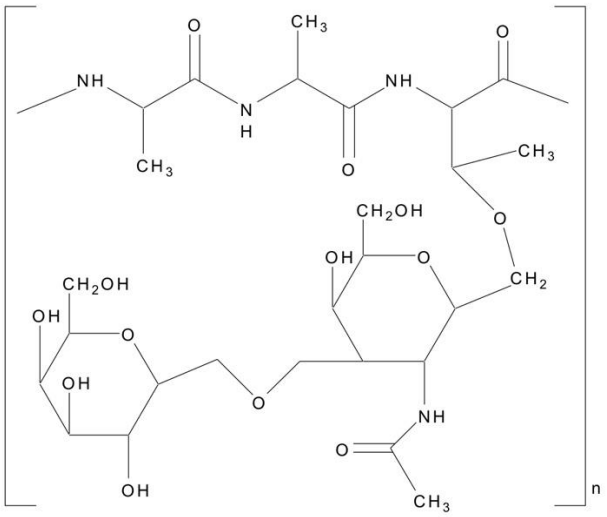

Figure 2.12 Structural unit of anti-freeze protein.

For optimal performances, the ideal molecular weight for a KHI polymer is around *1500-3000 g/mol* (Del Villano 2009). A molecular weight below *1000 g/mol* will cause the performance of the KHI to rapidly drop. At increasing molecular weights above 3000 the performance drops slowly but doesn't disappear. A low molecular weight polymer has the added advantage of keeping the viscosity low, which is beneficial for the flow (Del Villano 2009). The polymerization procedure, such as the temperature, monomer residence time in the reaction mixture and the solvent, may also play a part in the tacticity of the polymer. This statement has been shown for poly(N,N-dialkylacrylamide)s (Kelland 2012). There are three basic tacticities, Figure 2.13, that can form in varying amount for polyvinyl polymers. Isotactic, where all side chains are oriented on the same side of the polymer backbone. Syndiotactic, alternating up-down orientation of the side chain. Lastly there is atactic, where random orientation of the side chains occurs.

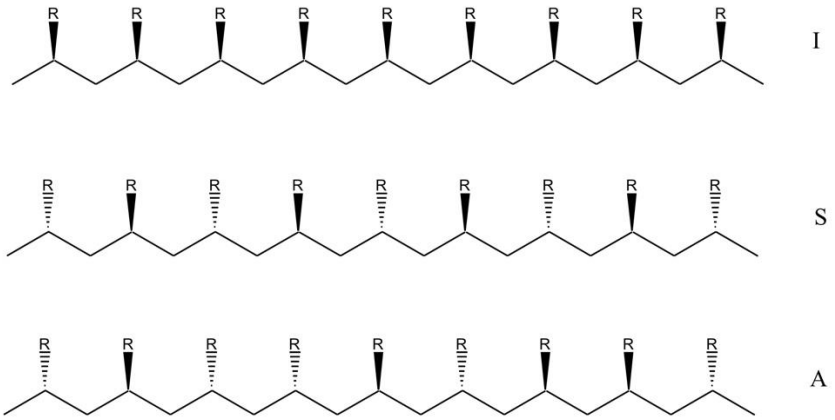

Figure 2.13 Structures of isotactic (I), syndiotactic (S) and atactic (A) PV-polymers.

Polymers with 100% syndiotacticity or isotacticity were made with site-specific zirconium catalysts, whereas atactic polymers were med using radical polymerization with azo or peroxide chemicals (Kelland 2012 and Chen 2010). By using high pressure isothermal stirred autoclave test with a sII hydrate-forming gas, it was shown that isotactic polyacryloylpyrrolidine (PAP) have shorter induction times than atactic PAP. These observations can be rationalized, by the assumption that the primary nucleation inhibition mechanism is disturbed by water structure, in that the side groups in isotactic PAP are more crowded together than atactic PAP. This results in less water disturbance for the isotactic PAP and has therefore less effect on disrupting hydrate nucleation. On the other side, isotactic PAP gave longer periods of slow hydrate growth compared to atactic PAP. The reason could be that the isotactic PAP has a higher concentration of side groups on one side of the PV backbone than atactic PAP. This may give isotactic PAP better adsorption onto the growing hydrate crystal surfaces.

2.4.3.1 Factors affecting KHI performance

There are many factors that can affect the KHI performance. This can be everything from the structure of the hydrate to the polymers and its characteristics.

First up we have hydrate categories. Methane gas from structure I hydrates as the most thermodynamically phase, and SNG form structure II hydrates. It was reported by Semenov et al. that Luvicap *55W* and Luvicap EG, both at *5000 ppm*, could by using the slow constant cooling method inhibit methane-propane sII hydrate the subcooling as high as *13-14 ℃*. But both KHIs were only capable of inhibiting methane sI hydrates at subcooling below *7 ℃* (Semenov et al. 2016). PVCap has been reported to be an efficient KHI on sII hydrates rather than on sI, probably due to sI hydrates form initially (Mozaffar et al. 2016). PVCap influences the structural transition of gas hydrates by disturbing the gas movement and the water rearrangement at the surfaces of hydrate crystals. It was observed that PVCap could promote the structural transition to stable sI hydrates, when thermodynamically stable conditions occur. It delays the structural transition to stable sII hydrates when it's in a thermodynamically phase (Sloan and Koh et al. 2009). This could explain why structure I hydrates are harder to inhibit than structure II hydrates.

As mentioned earlier, the ideal molecular weight for a KHI polymer for optimal performance is around *1000 – 3000 g/mol*. KHI monomers have little inhibition effect on hydrate formation, and the performance of a polymer increases with increasing repeating units, until an optimum size is reached, and then it decreases gradually with a longer polymer chain. This indicates that a KHI polymer with 8-20 monomer units have the best KHI performance (Chua and Kelland 2012). It was patented that KHI performance of polymers with a bimodal distribution of molecular weight is better than polymers with unimodal molecular weight distribution polymers. Yagasaki came up with a model explaining why KHI polymers have an optimum size, and why polymers with bimodal molecular weight distribution perform better via molecular dynamics (Yagasaki et al. 2018). They proposed that a molecule can be a good KHI only if it could strongly bind to hydrate surface. This is the reason VCap isn't considered a good KHI, as its monomers cannot inhibit hydrate growth since they are weakly bound molecules. On one hand, they have the ability of binding to the hydrate surface increases with the increasing repeating monomer units in PVCap from 1 to 20, and it remains the same if over 20 monomer units. On the other hand, the ability of binding to hydrate surface per monomer unit decreases with the increasing size of PVCap. An optimum size of PVCap will therefore occur before reaching 20 monomer units, because of the balance of the two opposite effects.

The polymerization method can affect the KHI polymers performance. By adding different chain transfers agents during the free radical polymerization process can polymers tailed with varying end-capping groups that change the polymers KHI performance (Zhang et al. 2017). Mercaptoacetic acid and mercaptoethanol end-capping groups were found to have positive effects on the KHI performance of PVCap. There could be a possibility that the end-capping groups change the activity of KHI polymers, or that themselves can directly work on the cavities of hydrates. As it was mentioned earlier in this section, tacticity influences KHI polymer performance.

For many polymers the KHI performance depends on the size and shape of the hydrophobic alkyl side groups. The optimum size is 3-6 carbon atoms, depending on the type and positions of the hydrophilic functional group. Hydrophobic groups with 7 or more carbon atoms are considered poor KHIs (Dirdal and Kelland 2019). The KHI performance increases with ring size for the poly (N-vinyl lactam) series, from 5 to 8-membered. The methyl groups on the backbone improve the KHI performance. It was shown that PIPMAM performed better than PIPAM (Colle et al. 1996), and that poly (N, N-dimethylhydrazidomethacrylamide) (PDMHMAM) performed better than poly (N, N-dimethylhydrazidoacrylamide) (PDMHAM) (Ree and Mady et al. 2015).

Cloud points are often seen when heating KHI aqueous solutions. This is because KHI formulations include one or more amphiphilic polymers. Low cloud point temperature is essential for efficient KHI performance (Dirdal and Kelland 2019). The reason being that KHI polymers with low cloud point have the maximum volume ratio. Another reason being they hydrophobic interaction of KHI polymers may be strengthened at low temperatures due to the low cloud point. Overall, KHI polymers with low cloud point tend to concentrate at the gas/oil-water interfacial regions, where hydrates may form and giving efficient inhibition performance.

Adding synergists to improve KHI performance is an efficient and money-saving method. It is especially advantageous if the carrier solvent for the KHI polymer is also a synergist. Typical synergists include small alcohols, alkyl lactates and glycol ethers, e.g. n-butyl glycol ether (nBGE) and iso-butyl glycol ether (iBGE), and some ketons (Ree and Kelland 2019). iBGE and nBGE were the two synergists used in this project and their effectiveness is discussed and shown later in this thesis. 4-methyl-1-pentanol was recently shown to be a powerful synergist (Kelland et al. 2020). The mechanism of the synergetic effect is still unclear. The synergists may enhance the reaction of KHIs on the hydrate surface, change the nucleus formation site or decrease the mass transfer rate of the hydrate formation system (Ree and Kelland 2019).

More factors can affect the KHI performance, apart from those mentioned above, such as KHI concentration, aqueous volume, stirring rate, test methods and experiment equipment (Kelland et al. 2000).

2.4.3.2 Performance testing of KHIs

Before a chemical is used in oil fields, several tests on the performance must be carried out. The reason being to better understand how the chemical´s inhibitions will act in different conditions, and how it potentially will affect the environment.

There has been, and still are, several testing methods to test the performance of KHIs. A common technique is the minimum hold-time (the duration when the system reaches the hydrate stability region and when hydrate formation starts) in worst-case subcooling field conditions is determined if an operator is interested in qualifying a chemical for field use (Klomp and Mehta 2007). Since the flowlines won´t always be at the same maximum subcooling and pressure, the result will give a conservative value of the dosage required to eliminate hydrate problems (Kelland 2009). For field verification under planes or unplanned shut-in conditions, shut-in test with no flow must be included. Experiments with the presence of other production chemicals should be run, since it’s known that many film-forming corrosion inhibitors may affect the performance of the KHIs negatively (Kelland 2009). Autoclaves, rocking cells, pipe wheel and loops are all testing methods used in which the test can be carried out with the fluid and gas composition of the actual field (Kelland 2014).

3 MATERIALS AND METHODS

3.1 Solutions and Chemicals

The tables under show an overview over the different chemicals and gasses used, as well as the PVAmOx syntheses made and tested.

The Lupamines were provided by BAFS.

Table 3.1 Overview of Lupamin polymers used in this project and their meolecular weight.

PVAm	**mW**
Lupamin 1595	Low, 10 wt% and 15 wt% in water
Lupamin 5059	Middle, 11 wt% in water
Lupamin 9095	High, 11 wt% water

Table 3.2 Overview of gases use and their composition.

Gas	**Producent**		**Content**
SNG (Synthetic Natural Gas)	NIPPON GASES	UN 1954	Gasmixture, 7 comp. C1-C4, Methane > 77% Methane, propane
Methane	YARAPRAXAIR	UN 1971	Methane 2.5, compressed

Table 3.3 Overview of the "Hoogenboom" polymers used in this project.

Hoogenboom Polymers	**Name of Polymer**
SJ192	PPiOx25-PPyOx25
SJ258	PPiOx27-PPyOx23
SJ244	PPiOx15-PPyOx12
SJ268	PPiOx10-PEI2-PPyOx13
SJ271	PPiOx12-PMoOx13
SJ272	PPiOx14-PMoOx11
SJ274	[PPiOx-PEI]25 (10 mol y * PEI)
SJ301	PPiOx20-PMoOx5

Table 3.4 Overview of the PVAmOx syntheses made and tested.

PVAmOx - synthesis	**Date made**	**mW**	**Extra**
PVAmBu_2O (Cecilie)			This solution was made by a previous bachelor student
Solid PVAmBu_2O	19.01.2024		
Liquid PVAmBu_2O	19.01.2024		
PVAmBu_2O	23.01.2024		

$PVAmPr_2O$	23.01.2024	Low	Tested a few days after being made
$PVAmBu_2O$	26.01.2024		
$PVAmBu_2O$	05.02.2024	High	
$PVAmBu_2O$-I	13.02.2024	Middle	
$PVAmBu_2O$-II	13.02.2024	Middle	
$PVAmBu_2O$	15.02.2024	Low	4x batch size (1.5mol extra BuBr + NaOH)
$PVAmBu_2O$ w/ acetonitrile	05.03.2024		
$PVAmBu_2O$ (Cecilie method)	05.03.2024		2 mol extra NaOH and 2.5 mol extra BuBr
$PVAmBu_3Br$	14.03.2024		
Michael addition	18.03.2024		Lupamin vacc down
$PVAmBu_3Br$ quat. w/ acetonitrile	20.03.2024		
PVAmBuO	22.03.2024		Monobutylated
$PVAmBu_2O$	05.04.2024		4x batch size
$PVAmBu_2O$	08.04.2024		4x batch size

3.2 Rocking Cell RC5

A Rocking Cell RC5, delivered by PSL Germany, was used as a testing instrument in this project. By using RC5, Figure 3.1, hydrate formation can be examined in the lab to test the effectiveness and efficiency of KHIs. The rig consists of 5 test chambers, they will be called cells from now on, with a volume of 40 mL in each cell. Each cell has sensors attached to the rig where temperature and pressure is measured. The cells are magnetically attached and can therefore easy be removed for filling and cleaning. The measuring principle of RC5 is based on the tilting of cool, pressurized cells. Inside each cell there is a metal ball, while testing its rolling over the length of the cells. With this kind of movement, the fluid-gas mixture blends, as well as the metal ball creates strong shear forces and turbulences inside the cells. By doing this the conditions in the pipelines are reproduced in the test cells. The 5 cells are placed on a movable axis in a cooling waterbath, a mixture of water and glycol was used. Time used for the whole test to preform can warry from 19 to 21 hours.

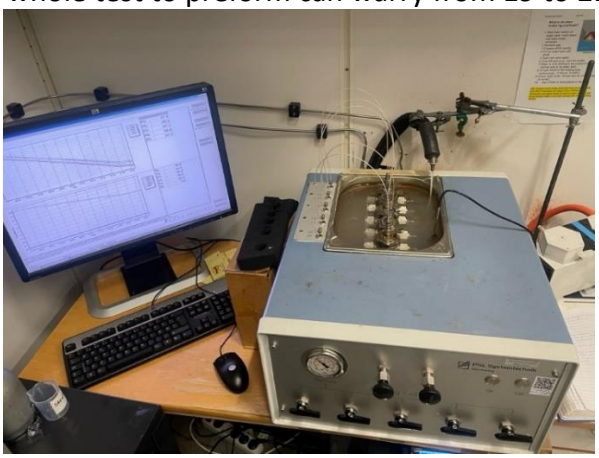

Figure 3.1 Set up for Rocking Cell RC5.

Under the Rocking Cell there is a cooler device, Figure 3.2, the cooling bath, where water circulates from the cooler into the cell waterbath and controls the temperature in the waterbath. This must be always filled with water, at least one centimeter from the top, or else there will be leaking and the waterbath will be empty causing the rocking of the cells to stop.

Figure 3.2 Cooling bath.

The Rocking Cell is connected to a computer, with a pre-installed PSL software called "WinRC", where we get the data from. The data comes in a form of a graph, Figure 3.3, where we can see the T_o and T_a values for all the cells. The top lines show the data of the pressure, whilst the bottom lines represent the temperature. The data is later transferred to a memory stick and opened in Excel where we can see the exact T_o and T_a values for each cell, Figure 3.2.

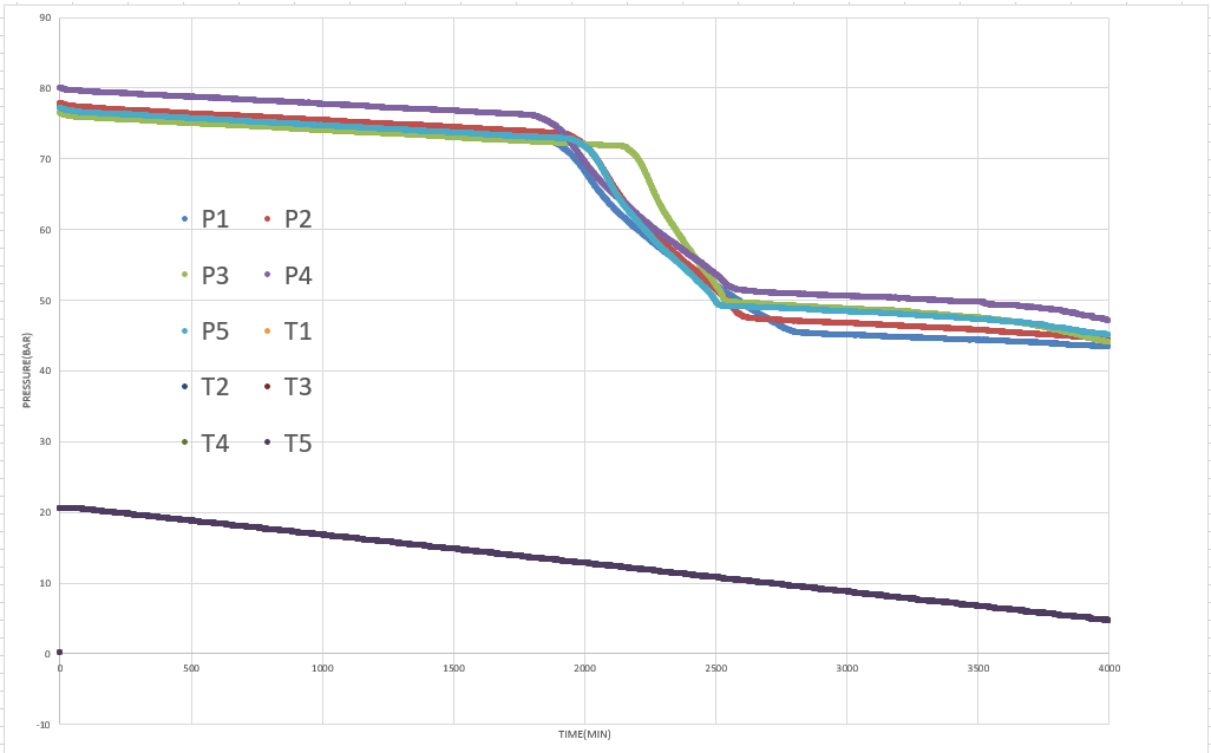

Figure 3.3 Example of how hydrate formation graph may look like for all 5 test cells.

T_o, the onset temperature, is where the first hydrate crystals form. T_a, ambient temperature, this is where the hydrate formation is the fastest. As seen in Figure 3.4 the T_o has a value of 13.5°C, whilst the T_a is 12.7°C. These values will be discussed later in the thesis. The goal is to have a T_o value lower than 10°C.

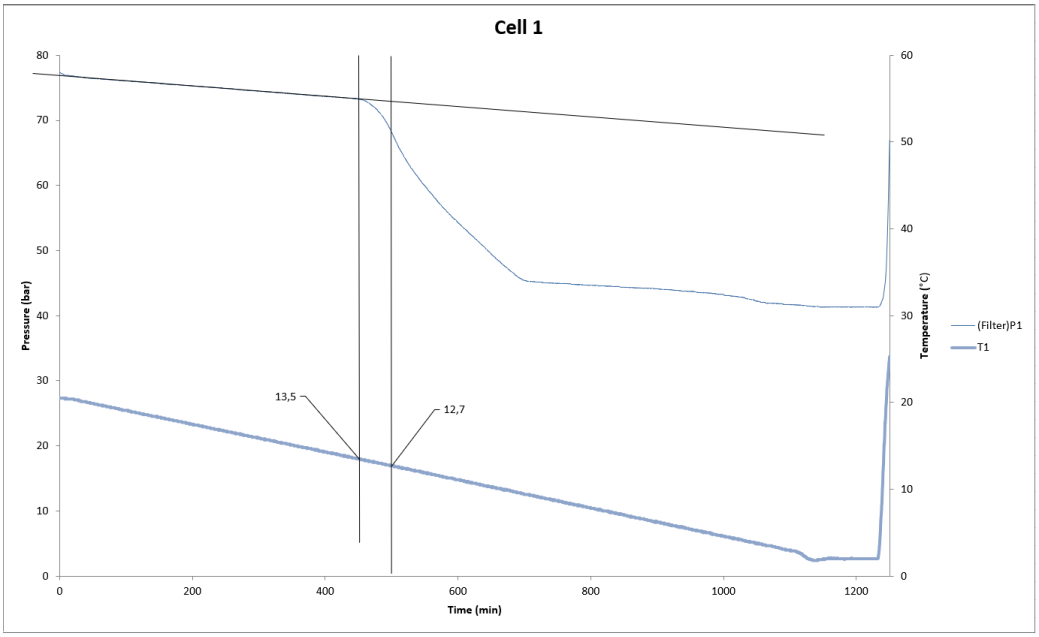

Figure 3.4 Example of hydrate formation for one individual cell.

Since the cells are filled with fluid, we must make sure that the cover caps are tightly closed so we don't lose any liquid product. For this a big spanner is used to close, and to open them afterwards, the cover caps.

When it comes to cleaning the cells, we have to make sure that they are thoroughly cleaned. This can affect the results of the following test if not, as well as it will pollute the next product used. When cleaning the cells, we follow a routine where we wash the cell, cap, and the metal ball:

1. Rinse the cells and wash with Zalo.
2. Tap water. Make sure to remove all the Zalo from the cells, also the hole where the sensors are connected to.
3. Acetone.
4. Tap water.
5. Distilled water.

The equipment is dried by using an air gun. This makes sure that there is no water left in the cells, so it won´t mess up the concentration of the products tested. The metal balls are also dried with an air gun.

This year we had access to two RC5-rigs, let's call them RC5-1 and RC5-2. Both rigs are set up the same and they work the same, only differences are type of gas and pressure added to

the cells. RC5-1 uses SNG, and the pressure is at 76 bar, whilst RC5-2 uses methane gas, and the pressure starts at 110 bar. The figure below shows the set up for RC5-2.

Figure 3.5 Set up of RC5-2.

We have had some problems with both rigs, mostly RC5-1 since it´s mainly and most used. We´ve had to remove some cells that were either not working or had some weird drops/values, as well as the RC5-1 cooling bath had a lot of leaking some period. The reasons why these problems occurred weren't obvious or know so we´ve had to work around them and continue with what we were able to do when problems occurred.

3.2.1 Test procedure

An introduction on how to use the Rocking Cell RC5 was presented by our PhD student so we could use it independently when testing the KHI performance of different solutions.

1. Before starting the test

Before we started with anything, we made sure that the cooling bath was on, the temperature of the waterbath was 20.5°C and that there was enough liquid in the cooling bath. For further use we marked each cell, and the cells cover cap from 1 to 5 so we´d know which cell were supposed to go where.

The metal ball was first added into the cells, otherwise there would be spillage if added later. When the cover lid was secured on the cell, we made sure that the cell was in a 45° angle, so the liquid wouldn't leak before we extra secured it with the spanner. The cell was then added in the waterbath and connected to the sensor. This was done with all 5 cells.

A plastic box, seen in Figure 3.5, was placed over the waterbath for safety reasons but since we had some problems with the cooling bath on RC5-1 we had to eventually stop doing this due to the water cable being able to lead the water into the waterbath. We made sure to use glasses when doing the test.

2. Pressurizing

Pressurizing the cells is repeated two times. First time this is done is to “flush” the cells, meaning that any air in the cells is taken out, and the second time is to reach optimal pressure before starting the test.

For flushing, make sure the “outlet”/ “inlet” valves on the Rocking Cell RC5 re closed, then:

a) Open valve on gas bottle.

On the “Gas Supply” Box:

b) Open “Gas 1” until reached pressure.
c) Close valve on gas bottle.
d) Turn compressor on to 120 outlet pressure.
e) Close “Gas 1” and “Gas out”.
f) Open “Gas out”.

On the RC5:

g) Open “inlet” valve and wait until pressure is reached between 10-20 bars. This can be seen on the WinRC software on the computer.
h) Close “Gas out” and “inlet” valve.
i) Click “Start motor” on WinRC software and wait 3-5 minutes before clicking “Stop motor”.
j) Turn gently on the “outlet” valve on the RC5 and wait until the pressure drops to zero. The pressure should drop with 1 bar per second.
k) Turn the vacuum pump on and vacuum for 3-5 minutes.
l) After this close the “outlet” valve.

For pressurizing to optimal pressure:

a) Open valve on gas bottle.
b) Open “Gas 1” until reached pressure.
c) Turn compressor on to 120 outlet pressure.
d) Open “Gas out” and “inlet” valve.
e) Close “Gas out”.
f) Repeat the steps above until it reaches 80 bars.
g) Click “Start motor” on WinRC software and wait 2 minutes before “Stop motor”.
h) Open “outlet” valve slowly until it reaches 76 bars, then close the “outlet” valve and valves on cells immediately.

If it goes below 76 bars, then the steps above must be repeated.

For RC5-2 open “Gas 2” on the gas supply box. As for the optimal pressure for “flushing” the cells the pressure should be between 20-40 bars, and for pressurizing it should reach 118 bars before the pressure is dropped down to 110 bars.

Depressurizing the cells:

a) When the test is done, the temperature is at 20.5°C, the valves for each cell can be opened. Already here the pressure will start to drop, but nothing dramatically.

b) Open “outlet” valve and wait until the pressure has reached zero.
c) Turn the vacuum pump on and wait 3.5 minutes before closing it.
d) Disconnect the sensors from the cells.

You´re now able to remove the cells safely and wash them before next round of testing.

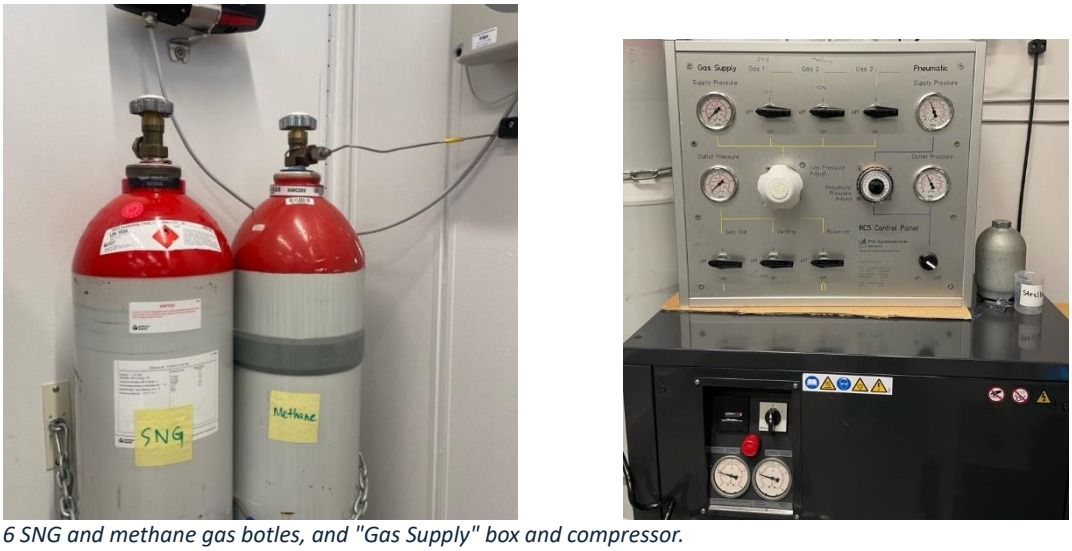

Figure 3.6 SNG and methane gas botles, and "Gas Supply" box and compressor.

3.3 Cooling Method

The performance of KHIs on gas hydrates can be tested by several methods:

1. The ramping method (Colle, Oelfk et al 1999; Del Villano, Kommedal et al. 2009).
2. Constant cooling method (Kellan, Svartås et al. 1994; Ajiro, Takemoto et al. 2010).
3. Isothermal method (Kellan, Svartås et al. 2000; Lee and Englezos 2006; Del Villano, Kommedal et al. 2008).

Constant cooling method was used in this project and will be presented in Chapter 3.3.1, Method 1 and 2 wasn’t used but will briefly be mentioned.

3.3.1 Constant cooling method

Constant cooling is performed by cooling the liquid in cells down to a very low temperature (high subcooling) (Del Villano and Kelland 2011). Water and inhibitors in this project were cooled down to 2°C. Typical graph from a constant cooling KHI can be seen in Figure 3.7. A large pressure drop can be observed when rapid hydrate formation ensues, this can also be seen in the two graphs under Chapter 3.2.

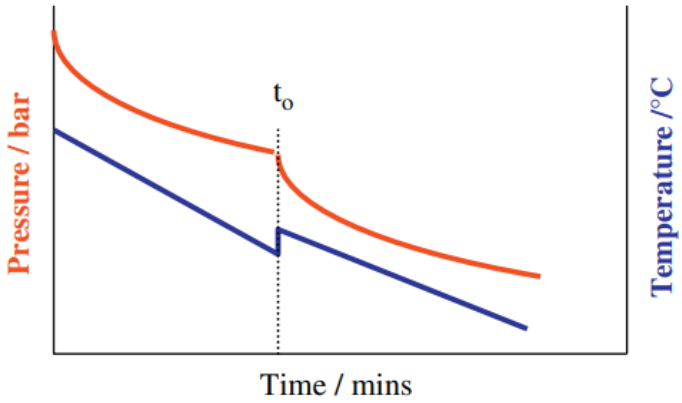

Figure 3.7 Typical graph from a constant cooling KHI (Del Villano and Kelland 2011).

The constant cooling is carried out in a closed vessel over a short period of time, and the induction time is difficult to determine since the pressure also drops due to the cooling of fluid (Del Villano and Kelland 2011). The induction time is an important characteristic of the kinetics in the system, as long induction time will allow transport of fluids through the production facilities to other processing plant without crystallization of hydrates in the system (Kashchiev and Firoozabadi 2002). Another name for the induction time is the nucleation delay time, and it is dependent om the subcooling in the system – higher subcooling gives lower induction time (Del Villano and Kelland 2011).

3.3.2 Isothermal method

The isothermal method is based on cooling down fluids to a certain subcooling with or without rocking. The fluids are held at this temperature for a certain time, until hydrates start forming (Del Villano and Kelland 2011). Induction time is the most important time to determine, since the goal is to totally avoid the possibility of hydrate crystals forming as they could build up in the pipelines and eventually form a plug (Del Villano and Kelland 2011).

3.3.3 The ramping method

This method is performed by stepwise cooling. Here the fluids are cooled to a certain subcooling and held there for a few hours, then rapidly cooled to a somewhat higher subcooling, and held there (Del Villano and Kelland 2011). This can be repeated several times until hydrates form.

3.4 Gas Hydrate Onset Temperature

The onset temperature, T_o, is defined as the temperature of a system being cooled at which hydrates are first detected (Sloan 2011). Hydrate nucleation and crystal growth may take place before a system reaches T_o. The T_o may be difficult to find, but by drawing a horizontal line following the pressure and see where it´s deviating from the horizontal line makes it easier to find, Figure 3.8.

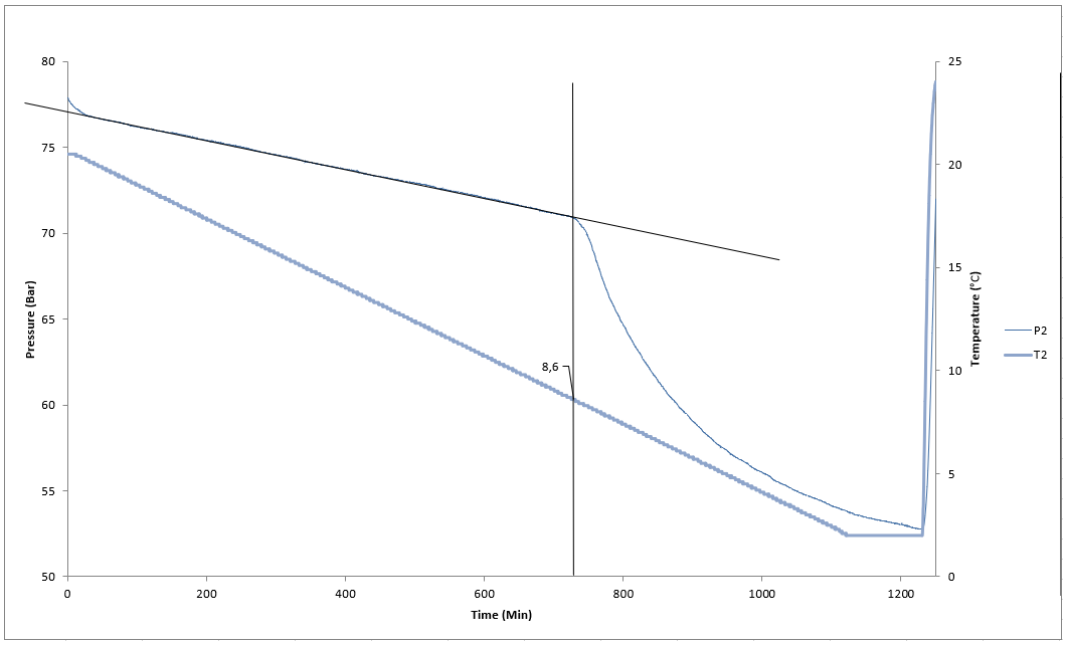

Figure 3.8 T_o for monobutyaled PVAmBuO 2500 ppm tested 22.03.24, cell 2.

3.5 Rapid Gas Hydrate Formation Temperature

After the first gas hydrates start to form is a snowball effect, and the formation will at a certain point reach its maximum. This point is called the point of rapid gas hydrate formation, T_a, and is found where the graph is the steepest. This is illustrated in Figure 3.9. The rapid gas hydrate formation temperature is found in the same way as the onset temperature.

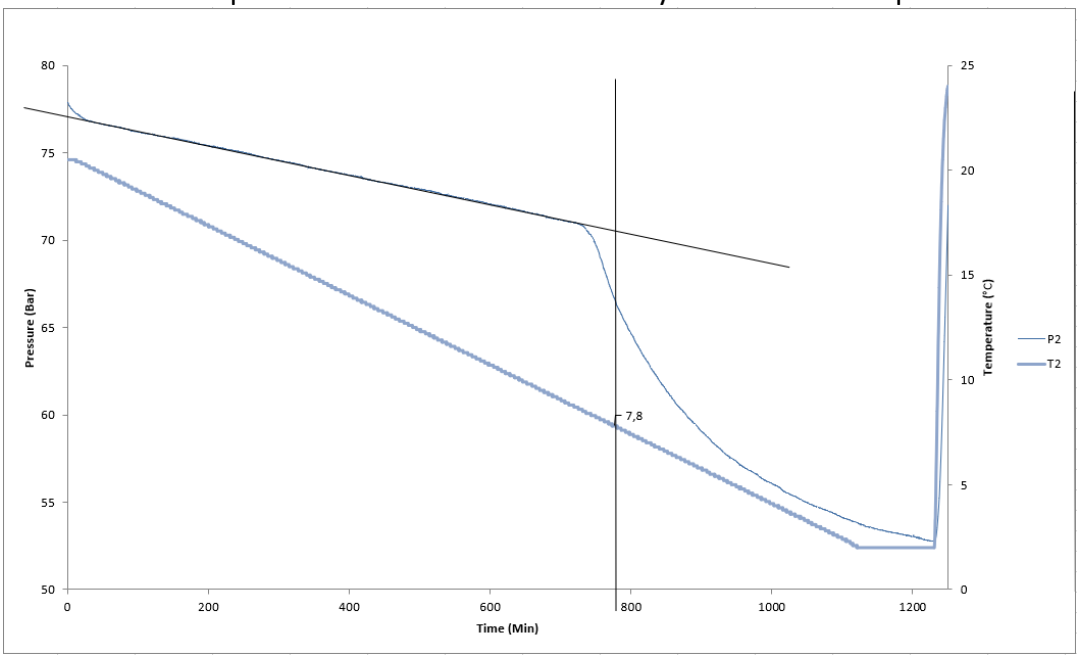

Figure 3.9 T_a for monobutyaled PVAmBuO 2500 ppm tested 22.03.2024, cell 2.

4 EXPERIMENTAL WORK

There were two projects done, the “Hoogenboom” project and “Polyvinyl amine Oxide syntheses”.

The “Hoogenboom” project was based on research done by Richard Hoogenboom and Malcolm A. Kelland with others. The polymers were delivered from Belgium and their KHI performance was tested with different concentrations and volumes, as well as some synergists were added to some of the polymers. The second project, Polyvinyl amine Oxide, was done by me and my lab partner. Different kinds of Polyvinyl amine Oxides were made by using different molecular weighted Lupamin, not all will be mentioned in this thesis, and tested their KHIs performances as well. The results are discussed in Chapter 5.

4.1 The “Hoogenboom” Project

In table 3.3 you get an overview of the polymers sent from Belgium that we tested the KHI performances of. Since this is a quite new project there isn’t quite much research done and information out. This polymer is a new subclass of amphiphilic polymers, named poly(2-dialkylamino-2-oxazoline) s (PAmOx), Figure 4.1, and they are also thermoresponsive (Hoogenboom et al. 2019). They comprise a tetraalkylurea structure, in which one of the nitrogens is a part of the backbone, which theoretically are based on polymerization of AmOx-monomers (2-dialkyl-2-oxazoline) and that’s why they are called PAmOx. Hoogenboom, and others, reported that the performance of the best Hoogenboom polymers at 2500 ppm was similar to the commercial KHI polymer, poly(N-vinyl caproloctam). It was also revealed that PAmOx cycloalkylamino side chains had the best performance, especially when both pendant pyrrolidine and piperidine rings were present (Hoogenboom and Kelland et al. 2024).

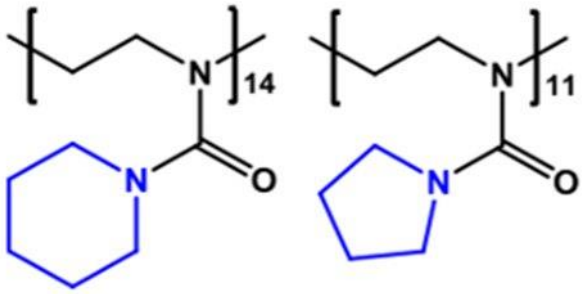

Figure 4.1 Example of a poly(2-dialkylamino-2-oxazoline).

The polymer concentration was made up by mixing deionized water with the polymer. This was done by mixing the polymer with water by using the equation to get the exact gram of polymer.

For *10000 ppm* polymer solution:

$$0.105L \times 10000\frac{mg}{L} \times \frac{1\ g}{1000\ mg} = 10.5\ g \text{ active ingredient (2)}$$

For *5000 ppm* polymer solution:

$$0.105L \times 5000\frac{mg}{L} \times \frac{1\ g}{1000\ mg} = 5.25\ g \text{ active ingredient (3)}$$

For *2500 ppm* polymer solution:

$$0.105L \times 2500\,\frac{mg}{l} \times \frac{1\,g}{1000\,mg} = 2.625\,g \text{ active ingredient (4)}$$

For *1000 ppm* polymer solution:

25 mL of 2500 ppm solution + 37.5 mL dH_2O (5)

After mixing water and the polymer in a beaker, a magnet was added and the solution stirred for 30 minutes, or at least till the polymer was dissolved.

The volume varies from the amount of volume used in each cell, 20 mL in all 5 cells equals to 100 mL and 10 mL in each cell equals to 50 mL. Always remember to add 5 mL extra to the volume in case some product gets lost due to spillage or condensation when solution is being stirred. 1000 ppm was never made from scratch, it was always diluted from 2500 ppm solution, but if it would be made from scratch then the same equation would be used. The 2500 ppm solution could sometimes also be diluted from a 5000 ppm solution, then we would take equal amount of 5000 ppm solution and dH_2O, e.g. 25 mL 5000 ppm and 25 mL dH_2O, to make the 2500 ppm solution.

4.2 Polyvinyl Amine Oxides syntheses

The amine group on a polymer is related to quaternary ammonium salts and to the amide group because of strong hydrogen-bonding properties (Bagley and Tovey 2001). Several polyamine oxides have been investigated as KHIs, and several show good KHI performance. The bonding in vinyl lactam polymers gives us an understanding of why the good performance. The enol tautomeric form of the lactam ring is more prevalent in VCap then it is in VP. This is because of the lower ring strain in PVCap and gives a higher degree and polarity on the oxygen atom of the caprolactam ring compared to pyrrolidone. As seen in Figure 4.2 the alkenol form has a negatively charged oxygen atom which can take part in stronger hydrogen bonding than a neutral oxygen atom (Kelland 2023).

Linear Polyvinyl amine oxides were mainly made. Other forms of PVAmOx were also tried to be made, like hyperbranched, and with other alkyl groups, e.g. propyl and pentane. Some were more successful than others and mainly PVDibutylamine oxides were made and tested. Table 3.4 shows an overview over the syntheses that were successfully made and tested, but some of the failed ones will also be mentioned.

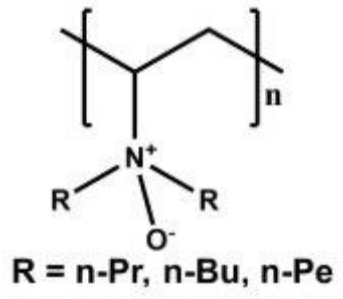

Figure 4.2 Amine oxide

4.2.1 Original synthesis of Polyvinyl(R) Amine Oxide

The whole process of the synthesis will be mentioned in this section to make it easier for further work.

There are different stages of making PVAmOx. We have the first stage where the first reaction happens, Figure 4.3. In this stage we mix all the products together to make the first product of this synthesis, PVAmR (R = alkyl group). The products used in the first stage are:

- Lupamin polymer
- dH_2O
- NaOH
- Isoburylnitrile (iPrCN)
- 1-Bromobutane or Butyl Bromide (BuBr)

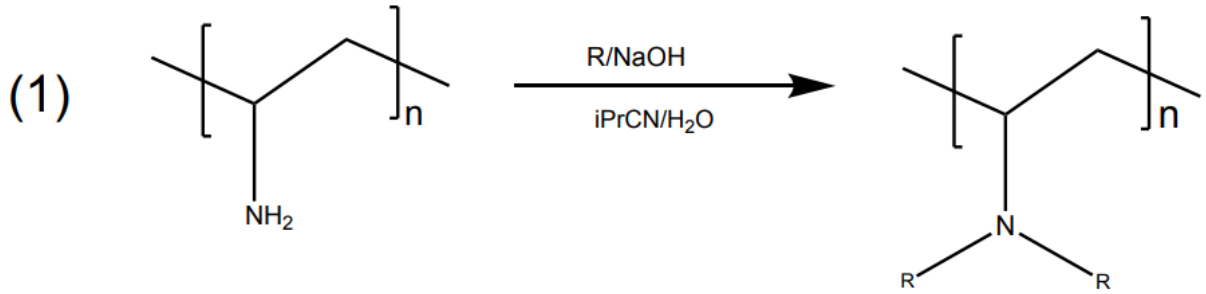

Figure 4.3 First stage of the PVAmOx synthesis.

Before the iPrCN is added to the solution NaOH has to be heated up and dissolved first, this is to make it easier for the products to react. After BuBr is added the solution is then refluxed overnight in an oilbath at either 71°C or 120°C, this will be specified for each synthesis mentioned. Figure 4.4 shows the setup for the reflux. There will already be two layers of product here, whom after the reflux will be separated.

Figure 4.4 Reflux setup.

4.2.1.1 Separation of Two Layers

After overnight reflux the two layers will have reacted with each other, and two new phases have been created a product -phase and a water-phase. The product-phase will always be the top layer, and it´s the layer we want.

After drying of the round bottom flask, the product is poured into a funnel, Figure 4.5 and separated. The water-phase is normally a clear colour, while the product-phase has some sort of color, e.g. light orange tint or dark brown. The reaction in the figure below didn't go as planned causing the water-phase to get a thick, slushy texture. As mentioned, the top layer is always wanted. The water and product-phase are both separated in two different beakers. The water-phase is added back to the funnel and washed with iPrCn. This is done to make sure that there isn't any product left in the water-phase since it can be a little hard to separate the two phases completely. After this the product-phase is then dehydrated with Na_2SO_4 to make sure there is no water in the product-phase.

Figure 4.5 Funnel with product-phase and water-phase.

4.2.1.2 Rotavap and Second Stage

After the separation the product is added to a florentine and put on the Rotavapor R-200, provided by BÜCHI. The setup is shown in Figure 4.6 Here the product is dried and vacced down by vacuuming.

The florentine is put on the Rotavap and steel hook secured, and the waterbath is heated up to 70°C. Whilst it´s being heated up the orange hoses are put into the pressure gauger and water runner. The florentine is sunk to the waterbath and the rotator turned on. Water is added slowly from the water course behind. Pressure is then added to the Rotavap, and the pressure hole is slowly being opened. This must be done slowly or else the vacuum can suck up the product in the florentine. When the product has been dried off for some time turn the rotating off, close the pressure hole and stop the water runner. Dry off the florentine and weigh it.

The procedure above is repeated until the weight of the florentine is stable.

Figure 4.6 Setup for Rotavapor R-200.

After a stable weight the second stage of the reaction can start, Figure 4.7. Here the oxidation happens due to the hydrogen peroxide, and we get our final product PVAmROx. For every *0.500 g* product 2-3 mL iPrOH is added to the dried product. As for the H_2O_2 the equation below is used to find the amount needed.

$$\frac{amount\ solid}{mw\ compund} \times \frac{mw\ H_2O_2}{wt\%\ H_2O_2} \quad (6)$$

H_2O_2 has a wt% of 30. $PVAmBu_2$ has a mW of *155 g/mol*.

This is stirred overnight in a beaker with a magnet.

The volume, concentration will vary from the values wanted. The wt% will vary from product to product. NB! The PVAmOx don't have the same wt%, this needs to be calculated.

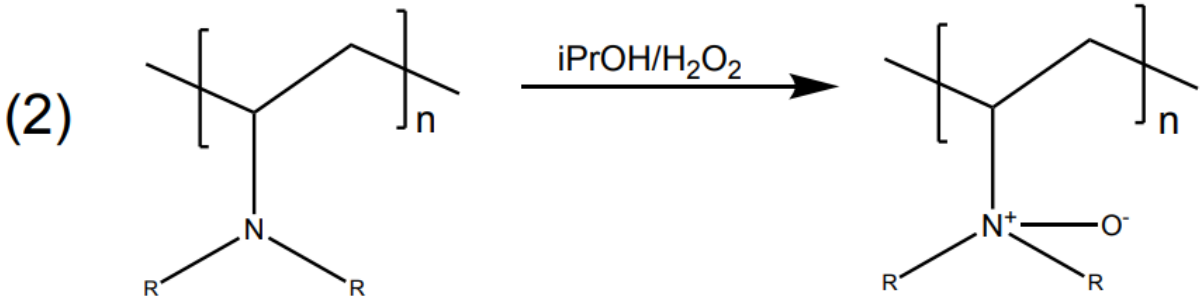

Figure 4.7 Second stage of PVAmBuOx synthesis.

4.2.1.3 Testing

When testing the PVAmROx the same procedure is done here as for testing the "Hoogenboom" polymers, only difference being that the wt% must be known for the test solution to be made. The wt% is found by using the equation:

$$wt\% = \frac{m(product)}{m(solution)} \times 100\% \quad (7)$$

When the wt% is found equation (8) and (9) are used to make the testing solution.

$$volume\ (L) \times concentration\ (\frac{mg}{L}) \times \frac{1\ g}{1000\ mg} = X\ g \text{ active ingredient} \quad (8)$$

$$G_{PVAmBu2O} = \frac{active\ ingredient}{(\frac{wt\%}{100})} \quad (9)$$

Volume and concentration in equation (8) will vary from the values needed, the same as for testing the "Hoogenboom" polymers.

The steps mentioned above are required to do to be able to make and test PVAmOx.

4.2.2 Polyvinyl(Dipropyl) Amine Oxide

Stage 1:
8.475 g of Lupamin 1595 (low mW, 10 wt% in water), 15 mL of dH_2O, 1.65 g of NaOH, 16 mL of iPrCN, and 16 mL of n-PrOH was added to a round bottom flask. The reaction mixture was refluxed overnight at 71°C with a stirrer. The same procedure described in 4.2.1 was followed. The solvent was separated and vacced down the next day, by following the procedure described in section 4.2.1.1 and 4.2.1.2. This gave 0.851 g product.

Stage 2:
2.24 mL of iPrOH and 0.621 g of 30% H_2O_2 was stirred at room temperature overnight to give $PVAmPr_2O$ with 15.33 wt%.

For testing the solution procedure described in 4.2.1.3 was followed.

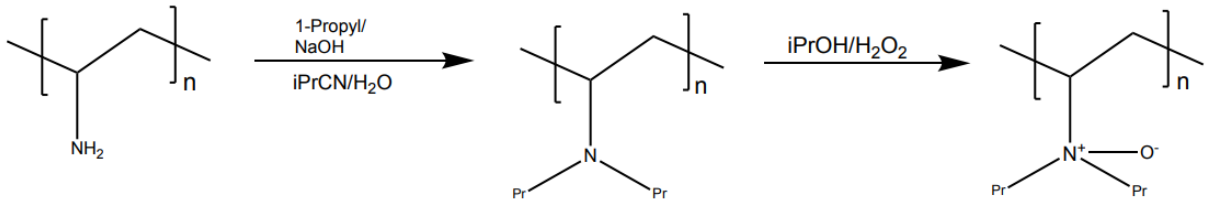

Figure 4.7 Two-stage synthesis of Polyvinyl(dipropyl) Amine oxide.

4.2.3 Polyvinyl(Dipentyl) Amine Oxide

Stage 1:
5.0 g of Lupamin 1595 (low mW), 10.072 g of dH_2O, 1.315 g of NaOH, 10.195 g of iPrCN and 3.810 g of 1-bromopentane was added to a round bottom flask. The reaction mixture was refluxed overnight at 71°C with a stirrer. The same procedure described in 4.2.1 was followed.

Since this was a new solution and never was tried made before it was unsure how it would work out. There was no product the next day, so NaCl was added to the product-solution, but it didn't seem to work. The product was left to reflux overnight again. On the third day there was 2 layers, and they were separated, and to the product-phase dH_2O, 13 mL of iPrCN and NaCl was added to get two new layers. This was left to settle overnight. On day four the two

phases were separated and vacced down, and procedures in 4.2.1.1 and 4.2.1.2 were followed. This gave 1.885 g product.

Stage 2:
16 mL iPrOH and 1.222 g of 30% H_2O_2 was stirred at room temperature to give PVAmPe_2O.

The solvent was regularly checked on throughout the day, and it was noticed that a lot of the product was on the sides of the florentine. This was tried to be pushed down into the solution but with no luck. The decision made was that this synthesis didn't work out.

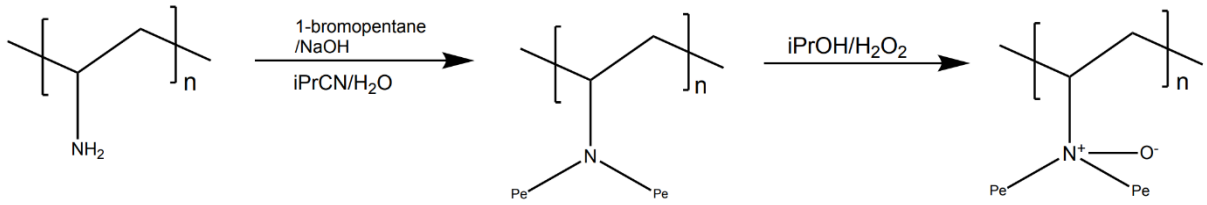

Figure 4.8 Two-stage synthesis of Polyvinyl(dipentyl) Amine Oxide.

4.2.4 High Molecular Weight Polyvinyl(Dibutyl) Amine Oxide

Stage 1:
10.672 g of Lupamin 9095 (high mW, 11 wt% in water), 19.726 g of dH_2O, 2.631 g of NaOH, 20 mL of iPrCN, and 6.692 g of BuBr was added to a round bottom flask. The reaction mixture was refluxed overnight at 71°C with a stirrer. The same procedure described in 4.2.1 was followed. The solvent was separated and vacced the next day, by following the procedure described in section 4.2.1.1 and 4.2.1.2. This gave 5.391 g product.

Stage 2:
10.2 mL of iPrOH and 1.617 g of 30% H_2O_2 was stirred at room temperature overnight to give PVAmBu_2O with 18.01 wt%.

For testing the solution procedure described in section 4.2.1.3 was followed.

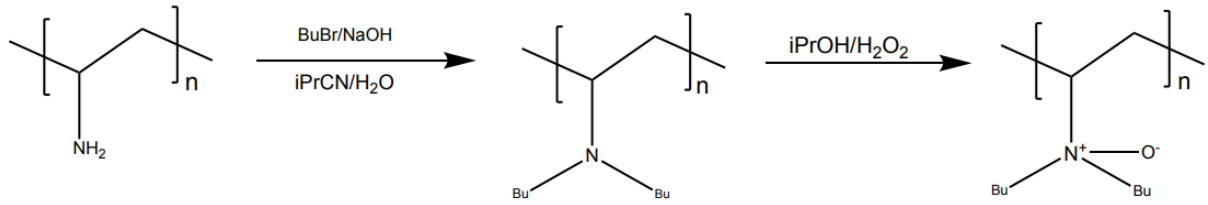

Figure 4.8 Two-stage synthesis of high mW Polyvinyl(dibutyl) Amine Oxide.

4.2.5 Big Batch Low Molecular Weight Polyvinyl(Dibutyl) Amine Oxide

Stage 1:
20.026 g of Lupamin 1595 (low mW, 10 wt% in water), 40.011 g of dH_2O, 5.215 g of NaOH, 40.0142g of iPrCN, and 13.500 g og BuBr was added to a round bottom flask. The reaction mixture was refluxed overnight at 71°C with a stirrer. The same procedure described in 4.2.1

was followed. The solvent was separated and vacced down, by following the same procedure described in section 4.2.1.1 and 4.2.1.2. This gave 4.095 g product.

Step 2:
13 mL iPrOH and 3.413 g of 30% H_2O_2 was stirred at room temperature overnight to give PVAmBu_2O with 18.24 wt%.

For testing the solution procedure described in section 4.2.1.3 was followed.

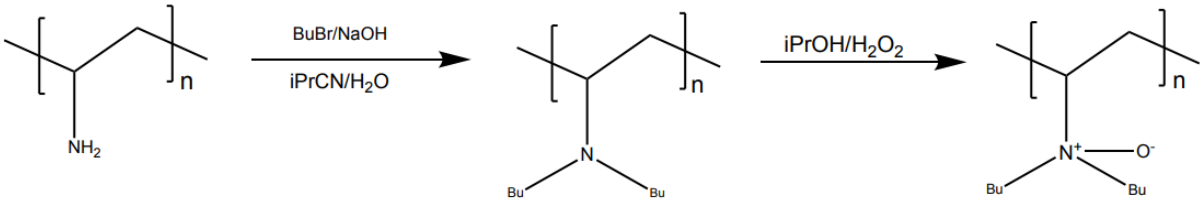

Figure 4.9 Two-stage synthesis of big batch low mW Polyvinyl(dibutyl) Amine Oxide.

4.2.6 Middle Molecular Weight Polyviny(Dibutyl) Amine Oxide

Stage 1:
20.074 g of Lupamin 5059 (middle mW, 11 wt% in water), 40.423 g of dH_2O, 5.224 g of NaOH, 40. 011 g of iPrCN, and 13.427 g of BuBr was added to a round bottom flask. The reaction mixture was refluxed overnight at 71°C with a stirrer. The same procedure described in 4.2.1 was followed.

This reaction didn't go as planned as well since it ended up with a slimy texture. Dichloromethane was added to dissolve the texture. This worked a little and gave 0.4 g product, but there was still more slime. Ethyl acetate was then added to the mixture, and this gave a slushy texture. 38.5 mL iPrCN was added to the slushy mixture and the product was vacced down by following the procedure described in 4.2.1.2. This gave 0.537 g.

Stage 2:
4 mL iPrOH and 0.412 g of 30% H_2O_2 was stirred at room temperature overnight to give PVAmBu_2O with 9.81 wt%.

For testing the solution procedure described in section 4.2.1.3 was followed.

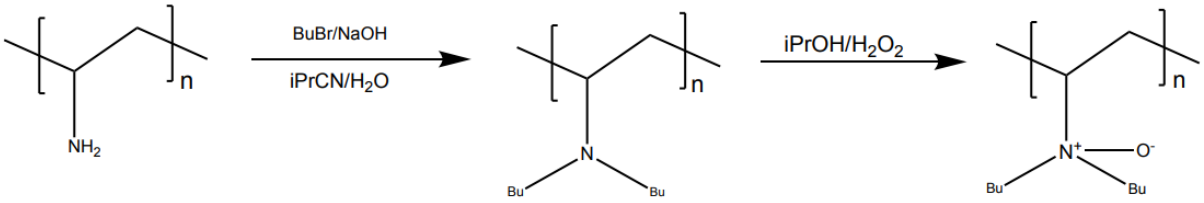

Figure 4.10 Two-stage synthesis of middle mW Polyvinyl(dibutyl) Amine Oxide-

4.2.7 Polyvinyl(Dibutyl) Amine Oxide with 1.5 mol NaOH and BuBr and Heptane Extract

In this synthesis the original amount of NaOH and BuBr was multiplied with 1.5 mol.

Stage 1:
20.023 g of Lupamin 1595 (low mW, 10 wt% in water), 40.030 g of dH_2O, 7.825 g of NaOH, 40 mL of iPrCN, and 20.648 g of BuBr was added to a round bottom flask. The reaction mixture was refluxed overnight at 71°C with a stirrer. The same procedure described in 4.2.1 was followed. The solvent was separated and vacced down the next day by following the procedure described in 4.2.1.1 and 4.2.1.2. Since the color of the solution was dark brown, an NMR was taken, and it didn't look good. The ^{1}H-NMR spectra can be seen under the appendices. A small amount of heptane was added to the brown solution which made it to one phase. The heptane was decanted out before rotavaping again. The solution still had some heptane extract the next day, so this was dissolved in iPrOH and vacced down again. This gave 3.353 g product.

Stage 2:
8.65 g of iPrOH and 2.571 g of H_2O_2 was stirred at room temperature overnight to give $PVAmBu_2O$ with 19.66 wt%.

For testing the solution procedure described in section 4.2.1.3 was followed.

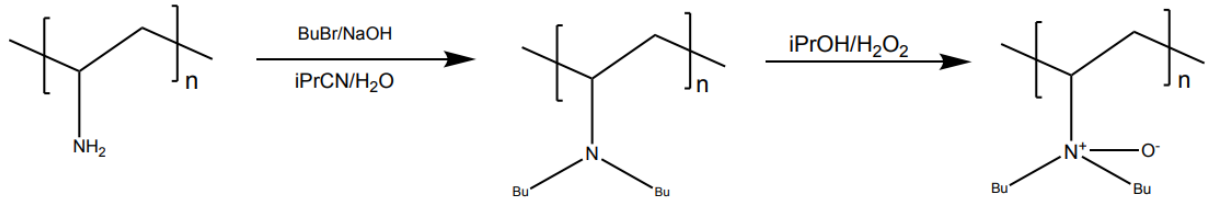

Figure 4.11 Two-stage synthesis of Polyvinyl(dibutyl) Amine Oxide with 1.5 mole NaOH and BuBr, and heptane extract.

4.2.8 Polyvinyl(Dibutyl) Amine Oxide with $NaHCO_3$

Stage 1:
10 g of Lupamin 1596 (low mW, 10 wt% in water), 20 g of dH_2o, 5.476 g of $NaHCO_3$, 20 mL of iPrCN, and 6.692 g of BuBr was added to a round bottom flask. The reaction mixture was refluxed overnight at 71°C with a stirrer. The same procedure described in 4.2.1 was followed. The solvent was separated the next day by following the procedure described in 4.2.1.1, only this time iPrCN. The solution was warm, which indicated it being an exothermic reaction. $NaSO_4$ was added instead, and the solution was vacced down, but the weight remained the same.

The conclusion being it didn't work because of a weak base.

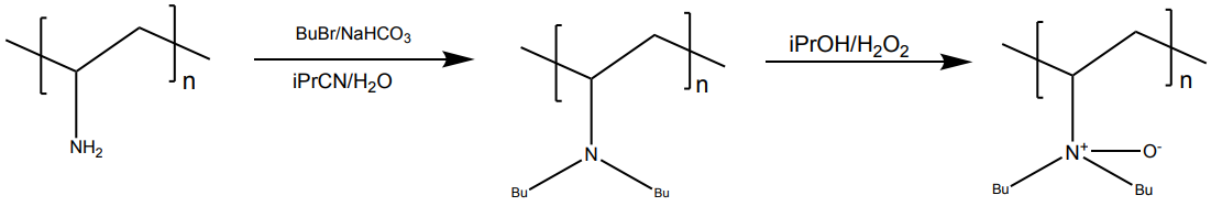

Figure 4.12 Two-stage synthesis of Polyvinyl(dibutyl) Amine Oxide with $NaHCO_3$.

4.2.9 Polyvinyl(Dibutyl) Amine Oxide with Acenonitrile

Stage 1:
10 g of Lupamin 1595 (low mW, 10 wt% in water), 20 g of dH_2O, 1.304 g NaOH, 20 mL of acetonitrile, and 3.346 g BuBr was added to a round bottom flask. The reaction mixture was refluxed overnight at 71°C with a stirrer. The same procedure described in 4.2.1 was followed. The mixture was made earlier on the day, and after a few hours of refluxing extra 7 mL of BuBr was added. The solvent was separated and vacced down the next day, by following the procedure described in 4.2.1.1 and 4.2.1.2. This gave 2.743 g product.

Stage 2:
7.32 g of iPrOH and 2.072 g of 30% H_2O_2 was stirred in room temperature overnight to give $PVAmBu_2O$ ^{w}/ acetonitrile with 13.9 wt%.

For testing the solution procedure described in section 4.2.1.3 was followed.

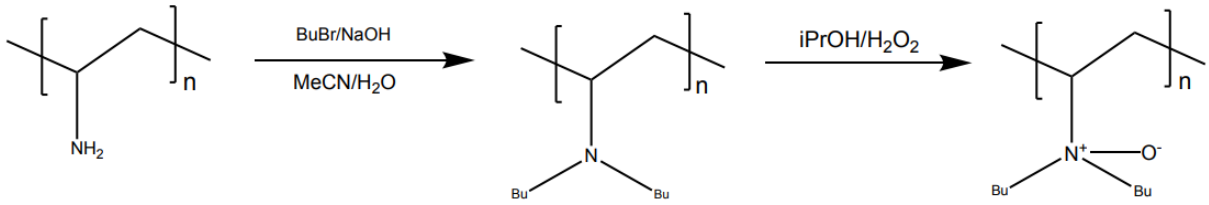

Figure 4.13 Two-stage synthesis of Polyvinyl(dibutyl) Amine Oxide with MeCN.

4.2.10 Polyvinyl(Dibutyl) Amine to Polyvinyl(tributyl) Amine

The ratio between NaOH and BuBr in this synthesis was 2.5 mol NaOH : 6 mol BuBr.

Stage 1:
10 g of Lupamin 1595 (low mW, 10 wt% in water), 20 g of dH_2O, 3.26 g of NaOH, 19.5 mL of iPrCN, and 20.076 g of BuBr was added to a round bottom flask. The reaction mixture was refluxed for 2 days at 120°C with a stirrer. The procedure described in 4.2.1 was followed. An extra 5 mL of BuBr was added to the mixture the next day while still refluxing. Later on, the same day the solution was separated and vacced down by following the procedures in 4.2.1.1 and 4.2.1.2. This gave 6.652 g product.

Stage 2:
23 mL of iPrOH was stirred in room temperature overnight to give $PVAmBu_3$ with 32.5 wt%.

For testing the solution procedure described in section 4.2.1.3 was followed.

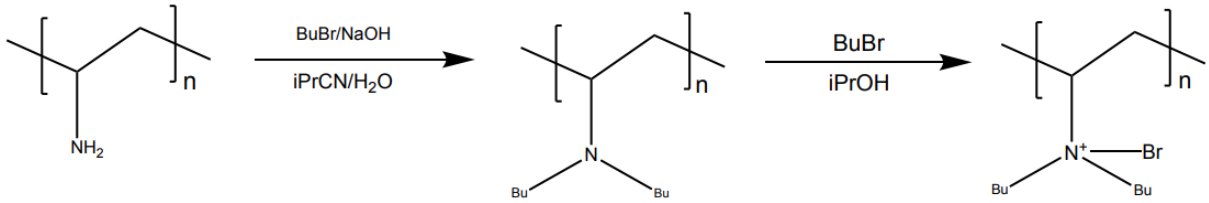

Figure 4.14 Two-stage synthesis of Polyvinyl(tributyl).

4.2.11 Monobutylated Polyvinyl Amine Oxide

Stage 1:
10 g of Lupamin 1595 (low mW, 10 wt% in water), 20 g of dH_2O, 1.304 g of NaOH, 20 mL of iPrCN, and 3.346 g BuBr was added to a round bottom flask. The reaction mixture was refluxed overnight at 120°C with a stirrer. The procedure described in 4.2.1 was followed. The solution was separated and vacced down the next by following the procedure described in 4.2.1.1 and 4.2.1.2. This gave 0.786 g product.

Stage 2:
3 mL of iPrOH and 0.944 g of 30% H_2O_2 was stirred in room temperature overnight to give PVAmBuO with 20.24 wt%.

For testing the solution procedure described in section 4.2.1.3 was followed.

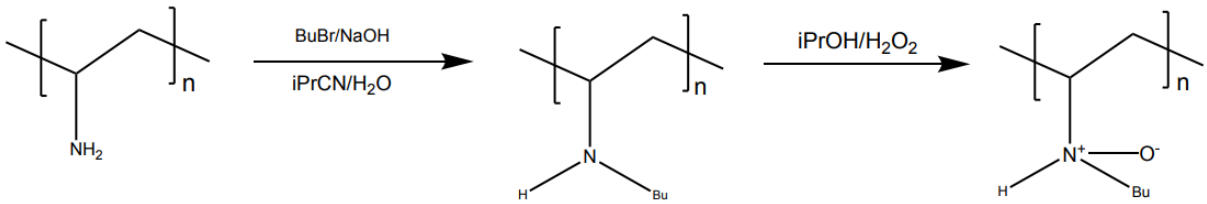

Figure 4.14 Two-stage synthesis of Monobutylated Polyvinyl Amine Oxide.

4.3 Other syntheses

Other syntheses were done in addition to PVAmOx syntheses. These will be mentioned below.

4.3.1 Synthesis of N-isopropyl-3-(isopropylamino) Propanamide(SAM3i)

Stage 1:
5 g of NIPAM (44.18 mmol) was degassed under high vacuum pump followed by purging under nitrogen three times and then dissolved in 43.08 g iPrOH. 3.13 g isopropylamine was added to the mixture under stirring. The reaction mixture was refluxed for 2 days at 80°C. the solvent was vacced down the next day and an NMR was taken. The ^{1}H-NMR can be seen in the appendices. This gave 7.938 g product.

Stage 2:
9.673 mL of Net_3 (69.35 mmol) and 80 mL CH_2Cl_2 was added to the mixture. The mixture was cooled under nitrogen atmosphere using an ice bath. The solution got a brown colour to it. To extract the product the filtering-method was used, with CH_2Cl_2 to wash the solid to get more product. When there is no more product left the solid will go white. The solid was added into a florentine with a little more CH_2Cl_2 and vacced down. Some of the product was taken out afterwards and washed with ethyl acetate to get some crystallization. This was again vacced down and an NMR was made with $CDCl_3$. The ^{1}H-NMR can be seen in the appendices.
The solid on the filter weighed 8.4 g and turned out to be trietylamine chloride. This was again extracted with ethyl acetate and vacced down. A new NMR-test was made.

This synthesis was a little side project since the product isn't a KHI. More research needs to be done to get the desired product and polymer.

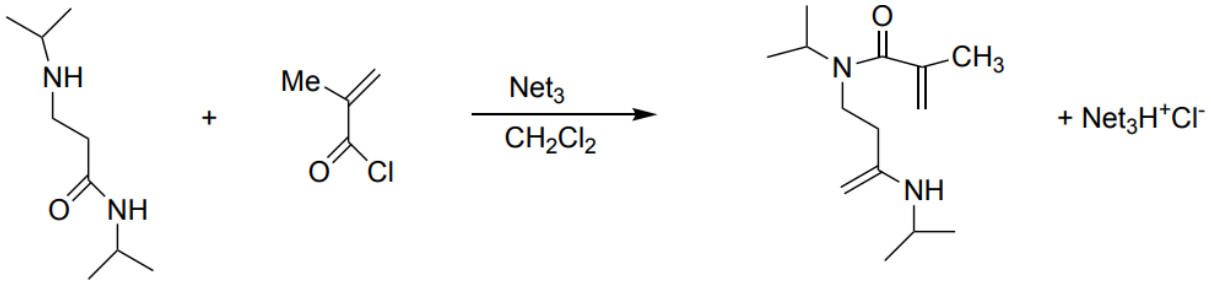

Figure 4.15 Synthesis of iPrNH₂.

4.3.2 Lupamin Vacc Down

20 g of Lupamin 1595 (low mW, 10 wt%) was added into a florentine and vacced down until it was dry. It was sealed with parafilm and put to the side.

After two weeks the dried Lupamin was weighed 7.549 g where around 2 g was active product. The product was then split in two beakers.

In one beaker the Michael addition was done.

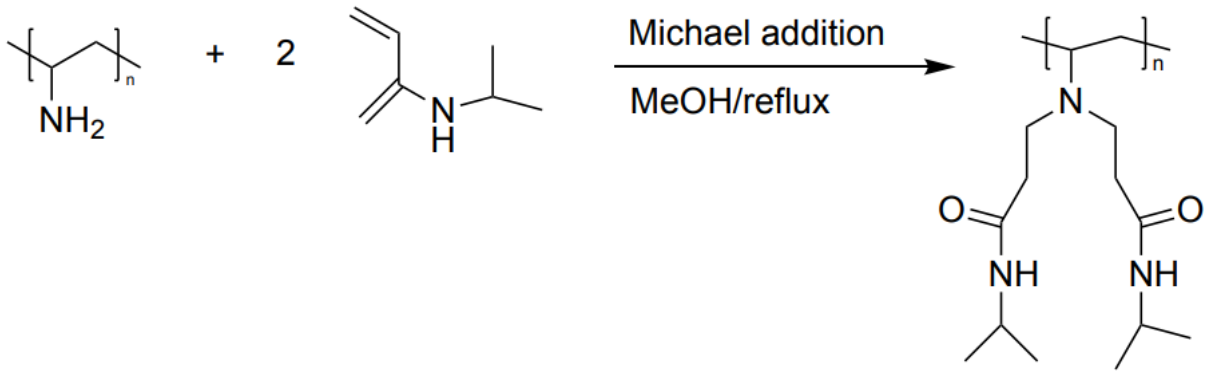

Figure 4.16 Synthesis done with <michael addition.

3.977 g NIPAM was added to the dried Lupamin, and 30 mL of methanol was refluxed overnight at 71°C with a stirrer. the solvent was rotavaped the next day. This gave 6.407 g product. This was put aside and later tested by following the procedure described in 4.2.1.3.

10 g of Lupamin 1595 (low mW, 10 wt% in water), 2.608 g of NaOH, 20 mL of iPrCN, and 6.692 g BuBr was added in the other beaker. The reaction mixture was refluxed at 120°C over 3 days. The solution was then vacced down by following the procedure in 4.2.1.2. This gave 3.885 g product.

For testing the solution procedure described in section 4.2.1.3 was followed.

5 RESULTS

In this section of the thesis there will be shown results for some of the polymers and products. These results will be described and compared to already known commercial KHIs. All results will be compared with water and PVCap. Water is not a good KHI at all, whilst PVCap is considered having one of the best KHI performance, and it`s also a common KHI used in the oil field.

5.1 $PVAmBu_2O$ vs. H_2O and PVCap

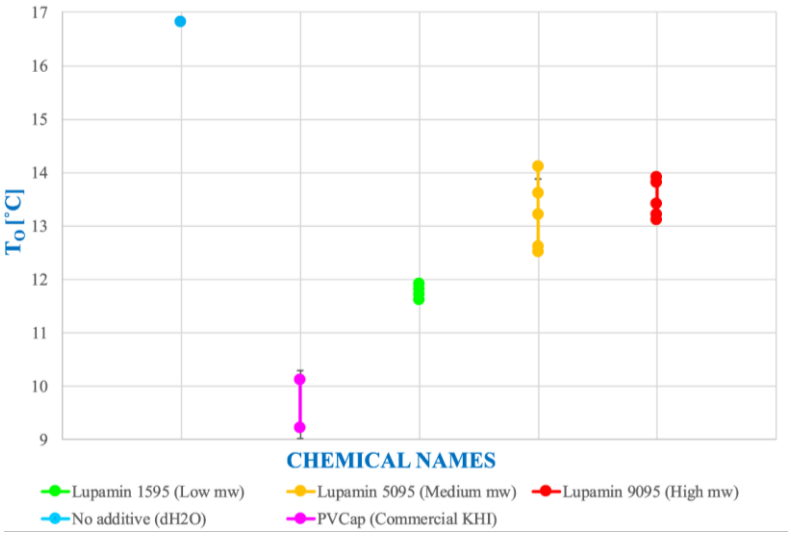

Graph 5.1 T_o for different molecular weighted Lupamines used in PVAmBu2O syntheses.

Mentioned earlier in this thesis was that the main goal with KHIs is to get a T_o at 10°C or under. Graph 5.1 shows a comparison of the different Lupamines, and the different mW, as well as PVCap. Seen from the graph is that Lupamin 1595 has best T_o. Already with this information it`s known that future work done with low mW Lupamin will have better results then middle and high mW Lupamin.

5.2 $PVAmBu_2O$ and different mW Lupamin

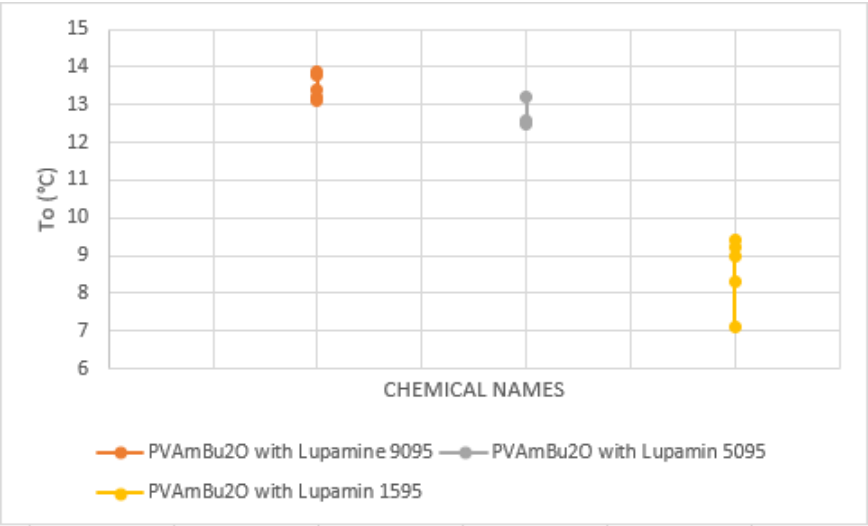

Graph 5.2 T_o for different mW $PVAmBu_2O$ in SNG.

The PVAmBu$_2$O made with low mW Lupamine, as expected, had a much better T_o compared to PVAmBu$_2$O with middle or high mW. The reason why will be discussed later.

5.3 Poly (2-dialkylamino-2-oxazoline) vs. H_2O and PVCap

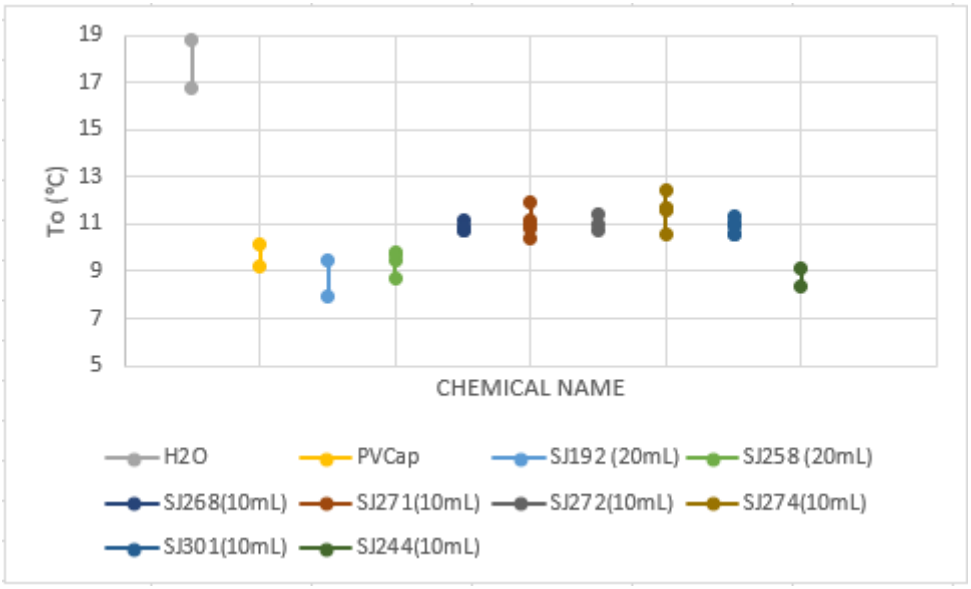

Graph 5.3 T_o for Poly (2-dialkylamino-2-oxazoline).

The KHI performance of Poly (2-dialkylamino-2-oxazoline) compared to water and PVCap. As seen 20 mL SJ192 had somewhat better values then PVCap.

5.4 Synergists

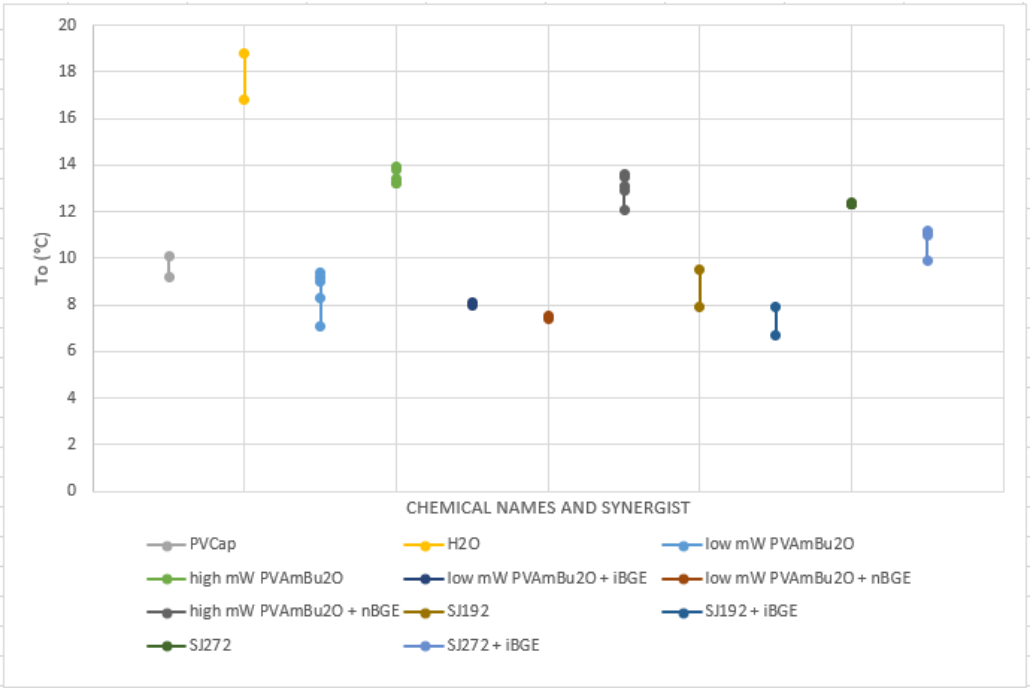

Graph 5.4 To for different polymers with and without synergists.

Synergists were added to a few polymers. The graph above shows the T_o value for some polymers with and without synergist. nBGE seemed to be the best working synergist with an average of 2.1°C.

5.5 Poly (2-dialkylamine-2-oxazoline) in SNG and Methane

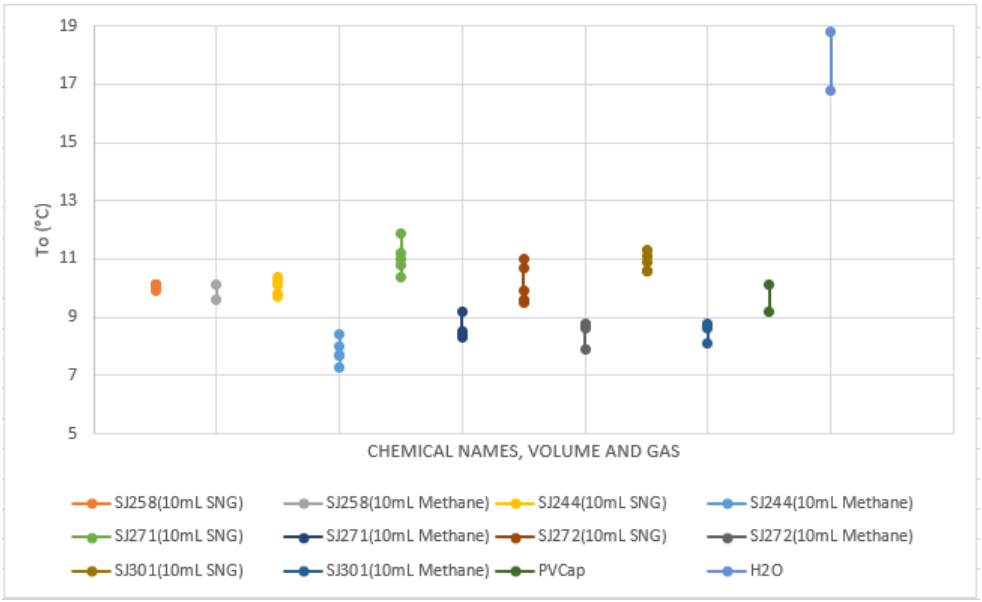

Graph 5.5 To for Poly (2-dialkylamine-2-oxazoline) in SNG and Methane.

Poly (2-dialkylamine-2-oxazoline) had different T_o values when tested in SNG compared to methane. Testing 10 mL Poly (2-dialkylamine-2-oxazoline) in methane at 2500 ppm showed far better performance than testing the same volume and concentration in SNG.

5.6 PVAmBu$_2$O in SNG and Methane

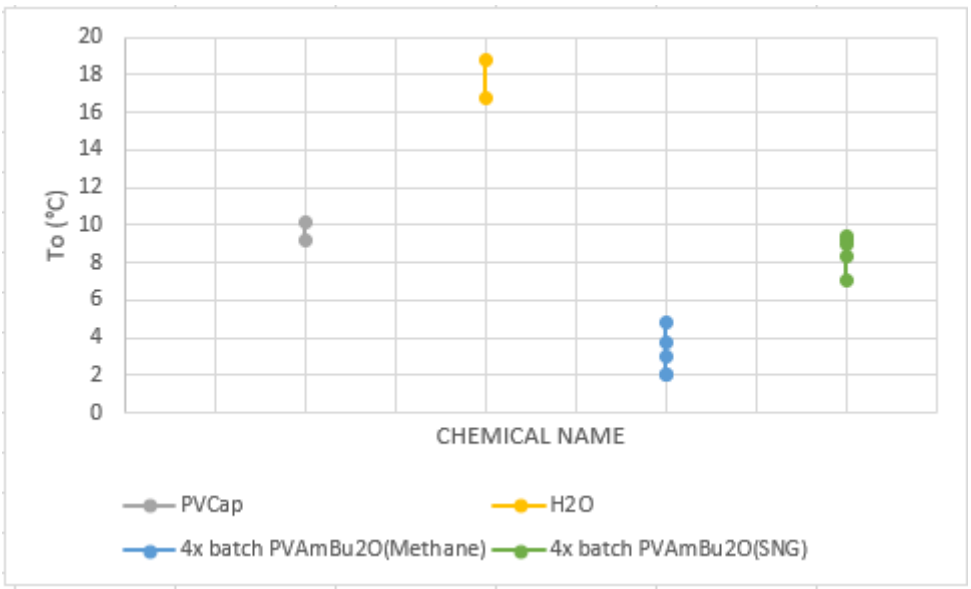

Graph 5.6 To for PVAmBu2O in SNG and Methane.

PVAmBu$_2$O showed far better performance in methane than in SNG.

6 DISCUSSION AND CONLUSION

When taking an overall look over the results and the T_o values, and comparing them with what is known today, some of the Poly (2-dialkylamine-2-oxazoline) and PVAmBu_2O had better values and performances then expected. Whilst some polymers impressed other didn't quite make the cut and had worse results than expected from them.

Molecular weight played a big role in the performance of the different KHI. As seen in Graph 5.1 and 5.2, lower molecular weight increases the performance by having a much lower T_o values then middle and high molecular weighted polymer. My theory on this is because of the large ratio between surface area and volume. Meaning that more inhibitors can connect to the hydrate crystal when the inhibitor has a lower molecular weight. This can be supported by research done on molecular weight improving KHI performances, where a low cloud point gives the maximum ratio of surface area to hydrodynamic volume ratio without losing water solubility (Dirdal and Kelland 2019).

Experiments done show that the gas hydrate inhibition is improved as the aqueous liquid volume increases. This can be seen in Graph 5.3, were SJ192 and SJ258 at 20 mL had better T_o value compared to the other polymers at 10 mL. This may be because a higher volume makes sure that the metal ball inside the rocking cells is covered in liquid and increases the efficiency of the rocking cells (Kelland and Dirdal 2021).

A concentration at 2500 ppm gave better results than 10000 ppm and 1000 ppm, some polymers with 5000 ppm worked better than those at 2500 ppm.

Section 5.5 and section 5.6 show the differences in T_o values for Poly (2-dialkylamine-2-oxazoline) and PVAmBu_2O tested in SNG and methane. As seen in Graph 5.5 and Graph 5.6 the T_o values were far much better in methane than SNG. The reason being in the subcooling. Methane gas is mostly used for structure 1 hydrates, while SNG for structure 2. The start pressure for methane was at 110 bar and the average T_o for Poly (2-dialkylamino-2-oxazoline) was at 8°C. This gives a subcooling at 7°C. For SNG the start pressure was at 76 bar and average T_o for Poly (2-dialkyl-2-oxazoline) was at 10°C, giving a subcooling at 9.5°C. Since SNG requires higher subcooling it will also have higher T_o values than methane.

As conclusion many of the Poly (2-dialkylamino-2-oxazoline) and PVAmOx reactions showed to be good inhibitors with great KHI performances, some better than expected even. Using the Rocking Cell RC5 is a great tool for KHI performances giving realistic and expected results. Salts like NaCl to increase the KHI performance seemed to work better than some synergist like nBGE and iBGE. My work at the lab took an end before I could join the testing with salts, but my lab partner gave me an inside scoop of the results.

As for further work and ideas, a blend with KHI and THI could be tested since both are good inhibitors. Even though proteins aren't favorable as synergists they should be tried since they can prevent from hydrates formatting further up the pipelines.

REFRENCES

Kelland, M. A.; Dirdal, E. G. Powerful Synergy of Acetylenic Diol Surfactants with Kinetic Hydrate Inhibitor Polymers - Choosing the Correct Synergist Aqueous Solubility. Energy Fuels 2021, 35 (19), 15721−15727.

Kelland, M. A.; Dirdal, E. G.; Ree, L. H. S. Solvent Synergists for Improved Kinetic Hydrate Inhibitor Performance of Poly(N-vinyl caprolactam). Energy Fuels 2020, 34, 1653−1663.

Sloan Jr., E.D., Koh, C.A., & Koh, C.A. (2007). Clathrate Hydrates of Natural Gases (3rd ed.).

Rachel O'Reilly; Nga Sze Ieong; Pei Cheng Chua; Malcolm A. Kelland Crystal growth inhibition of tetrahydrofuran hydrate with poly(N-vinyl piperidone) and other poly(N-vinyl lactam) homopolymers, Chemical Engineering Science, Volume 66, Issue 24, 2011, 6555-6560.

Amir Erfani; Farshad Varaminiam; Milad Mohammadi Gas hydrate formation inhibition using low dosage hydrate inhibitors, 2nd National Iranian Conference on Gas Hydrate (NICGH) 2014.

Bàez, L.A. and Clancy, P. (1994), Computer Simulation of the Crystal Growth and Dissolution of Natural Gas Hydrates. Annals of the New York Academy of Sciences, 715: 177-186.

Vatamanu J. Kusalik PG. Unusual crystalline and polycrystalline structures in methane hydrates. J Am Chem Soc. 2006 Dec 13;128(49):15588-9.

Yong Bai; Qiang Bai,15 - Hydrates, Subsea Engineering Handbook (Second Edition), 2019, 409-434.

Sanya Du; Xiaomin Han; Liang Zheng; Shijun Qin; Muhammad Arif; Dongpeng Yan; Xiaohui Yu; Hui Li The Journal of Physical Chemistry C 2021 *125* (14), 7889-7897.

E. D. Sloan; S. Subramanian; P. N. Matthews; J. P. Lederhos, and A. A. Khokhar Industrial & Engineering Chemistry Research 1998 *37* (8), 3124-3132.

Yongji Wu; Yurong He; Tianqi Tang; Ming Zhai. Molecular dynamic simulations of methane hydrate formation between solid surfaces: Implications for methane storage, Energy, Volume 262, Part B, 2023, 125511, 0360-5442.

Leo Kamiya & Ryo Ohmura (2024). Growth dynamics and morphology of D_2O + HFC-134a clathrate hydrate crystal toward tritiated water separation, Chemical Engineering Communications.

M.A. Kelland, T.M. Svartaas, and L.A. Dybvik Control of Hydrate Formation by Surfactants and Polymers. SPE 69th Annual Technical Conference and Exhibition, New Orelans, LA. 1994.

Malcolm A. Kelland. History of the Development of Low Dosage Hydrate Inhibitors. Energy & Fuels 2006 *20* (3), 825-847.

Erik Gisle Dirdal and Malcolm A. Kelland. Does the Cloud Point Temperature of a Polymer Correlate with Its Kinetic Hydrate Inhibitor Performance? *Energy & Fuels* **2019** *33* (8), 7127-7137.

Malcolm A. Kelland. A Review of Kinetic Hydrate Inhibitors – Tailor-Made Water-Soluble Polymers for Oil and Gas Industry Applications. 2012.

Halilburton. Low Dosage Hydrat Inhibitors. 2013.

Bagley M C, Tovey J. Diastereoselective synthesis of cis-2,5-disubstituted pyrrolidine N-oxides by the retro-Cope elimination[J]. *Tetrahedron Letters*, 2001, 42(2): 351-353.

Dimo Kashchiev, Abbas Firoozabadi. Induction time in crystallization of gas hydrates, Journal of Crystal Growth, Volume 250, 2003, 499-515.

Sloan E. D.; Koh C.; Sum K. A. Natural Gas Hydrates in Flow Assurance, 2011.
Luca Del Villano and Malcolm A. Kelland. An investigation into the laboratory method for the evaluation of the performance of kinetic hydrate inhibitors using superheated gas hydrates, Chemical Engineering Science, Volume 66, 2011, 1973-1985.
Radhakanta Ghosh and Malcolm A. Kelland. Pushing the Known Performance Envelope of Kinetic Hydrate Inhibitors—Powerful Synergy of Trialkylamine Oxides with Acrylamide-based Polymers, Energy & Fuels 2022 *36* (1), 341-349.
Ju Dong Lee and Peter Englezos. Enhancement of the performance of gas hydrate kinetic inhibitors with polyethylene oxide, Chemical Engineering Science, Volume 60, 2005, 5323-5330.
Del Villano, L., R. Kommedal, et al. (2009). Energy and Fuels 23.
Luca Del Villano, Roald Kommedal, and Malcolm A. Kelland. Class of Kinetic Hydrate Inhibitors with Good Biodegradability, Energy & Fuels 2008 *22* (5), 3143-3149.
Kelland, M. A., Svartaas, T. M., and L. Dybvik. "A New Generation of Gas Hydrate Inhibitors." Paper presented at the SPE Annual Technical Conference and Exhibition, Dallas, Texas, October 1995.
Mehta, A. P., Hebert, P. B., Cadena, E. R., and J. P. Weatherman. "Fulfilling the Promise of Low-Dosage Hydrate Inhibitors: Journey From Academic Curiosity to Successful Field Implementation." *SPE Prod & Fac* 18 (2003): 73–79.
Clark, Leonard W., Frostman, Lynn M., and Joanne Anderson. "Low Dosage Hydrate Inhibitors LDHI): Advances in Flow Assurance Technology for Offshore Gas Production Systems." Paper presented at the International Petroleum Technology Conference, Doha, Qatar, November 2005.
BASF. Low dosage Hydrate Inhibitors for the Oilfield Industry: Luvicap®. 2017.
PSL-Systemtechnik. (2011, 21.02.2011). "Research of Gas Hydrates with the Sapphire Rocking Cell." from PSL Systemtechnik: Laborgeräte und Messlabor für Erdöl, Erdgas: PSL Systemtechnik (psl-systemtechnik.com)
Dean Lovell, Conoco Canada and Marek Pakulski. SPE 75668. Calgary, Alberta, Canada 2002.
Kelland, M. A., T. M. Svartås, et al. (2008). "Gas Hydrate Anti-Agglomerant Properties of Polyproxylates and Some Other Demulsifiers." Journal of Petroleum Science and Engineering: 10.
Kashchiev, D. and A. Firoozabadi (2002). "Induction Time in Crystallization of Gas Hydrates." Crystal Growth.
Koh, C. A., R. E. Westacott, et al. (2002). "Mechanisms of Gas Hydrate Formation and Inhibition." Fluid Phase Equilibria 194-197: 9-
Lee, J. D. and P. Englezos (2006). Chemical Engineering Science 61: 1368-1376.
Del Villano, L. and M. A. Kelland (2009). An Investigation into the Gas Hydrate Precursor Test Method for the Laboratory Evaluation of the Performance of Kinetic Hydrate Inhibitors. Studies on Biodegradable Kinetic Hydrate Inhibitors. L. Del Villano. Stavanger, UiS.
Del Villano, L. and M. A. Kelland (2009). An Investigation into the Kinetic Hydrate Inhibitor Properties of two Imidazolium-Based Ionic Liquids on Structure II Gas Hydrates. Studies on Biodegradable Kinetic Hydrate Inhibitors. L. Del Villano. Stavanger, UiS.
Del Villano, L. and M. A. Kelland (2011). "An Investigation into the Laboratory Method for the Evaluation of the Performance of Kinetic Hydrate Inhibitors using Superheated Gas ……Hydrates." Chemical Engineering Science 66.

E. Dendy Sloan, J. (2003). "Fundamental Principles and Applications of Natural Gas Hydrates." Nature Vol 426.
Ajiro, H., Y. Takemoto, et al. (2010). Energy and Fuels 24: 6400.